Transcriptional repression induces a slowly progressive atypical neuronal death associated with changes of YAP isoforms and p73

Masataka Hoshino,[1] Mei-ling Qi,[1] Natsue Yoshimura,[1] Tomoyuki Miyashita,[2] Kazuhiko Tagawa,[1] Yo-ichi Wada,[1] Yasushi Enokido,[1] Shigeki Marubuchi,[1] Phoebe Harjes,[3] Nobutaka Arai,[2] Kiyomitsu Oyanagi,[2] Giovanni Blandino,[4] Marius Sudol,[5] Tina Rich,[6] Ichiro Kanazawa,[7] Erich E. Wanker,[3] Minoru Saitoe,[2] and Hitoshi Okazawa[1,2,8]

[1]Department of Neuropathology, Medical Research Institute and Center of Excellence Program for Brain Integration and Its Disorders, Tokyo Medical and Dental University, Bunkyo-ku, Tokyo 113-8510, Japan
[2]Tokyo Metropolitan Institute for Neuroscience, Fuchu, Tokyo 183-8526, Japan
[3]Neuroproteomics, Max-Delbrück Center for Molecular Medicine, 13092 Berlin, Germany
[4]Department of Experimental Oncology, Regina Elena Cancer Institute, 00158 Rome, Italy
[5]Weis Center for Research, Geisinger Clinic, Danville, PA 17822
[6]Department of Pathology, University of Cambridge, Cambridge CB2 1QP, England, UK
[7]National Center for Neurology and Psychiatry, Kodaira, Tokyo 187-8502, Japan
[8]Precursory Research for Embryonic Science and Technology, Japan Science and Technology Agency, Kawagoe, Saitama 332-0012, Japan

Transcriptional disturbance is implicated in the pathology of polyglutamine diseases, including Huntington's disease (HD). However, it is unknown whether transcriptional repression leads to neuronal death or what forms that death might take. We found transcriptional repression-induced atypical death (TRIAD) of neurons to be distinct from apoptosis, necrosis, or autophagy. The progression of TRIAD was extremely slow in comparison with other types of cell death. Gene expression profiling revealed the reduction of full-length yes-associated protein (YAP), a p73 cofactor to promote apoptosis, as specific to TRIAD. Furthermore, novel neuron-specific YAP isoforms (YAPΔCs) were sustained during TRIAD to suppress neuronal death in a dominant-negative fashion. YAPΔCs and activated p73 were colocalized in the striatal neurons of HD patients and mutant huntingtin (*htt*) transgenic mice. YAPΔCs also markedly attenuated Htt-induced neuronal death in primary neuron and *Drosophila melanogaster* models. Collectively, transcriptional repression induces a novel prototype of neuronal death associated with the changes of YAP isoforms and p73, which might be relevant to the HD pathology.

Introduction

Neurodegenerative disorders are characterized by the slow exacerbation of symptoms and by gradual progression of brain pathologies. Patients suffer for 5–20 yr from the onset of the disease to the bed-ridden state. Even fast-progressing amyotrophic lateral sclerosis takes 2–5 yr to render the patient bed ridden. Regarding the pathology, the total number of neurons and neural networks among them decrease. However, some of the neurons survive for an extensive period of time despite their expression of abnormal structures that are derived principally from the pathogenic disease-causing products. Typically, nigral neurons that express Lewy bodies in Parkinson's disease, hippocampal neurons that carry paired helical filaments in Alzheimer's disease, and motor neurons bearing Bunina bodies in amyotrophic lateral sclerosis can partially survive until the death of the patient. The mutant protein aggregates that characterize many of these diseases are known to trigger multiple cellular responses, including ER stress and mitochondrial abnormality. These stress responses are clearly sufficient to induce apoptosis in nonneuronal cell lines, whereas the brain pathology of patients indicates that neurons survive for a long period before their demise. A lengthy period of cell death is also observed in the polyglutamine (polyQ) diseases, a major group of neurodegeneration that includes nine disorders (for reviews see Gusella and MacDonald, 2000; Zoghbi and Orr, 2000; Ross, 2002; Taylor et al., 2002; Bates, 2003). Again, a fraction of the neurons that possess nuclear and/or cytoplasmic inclusions of mutant

Correspondence to Hitoshi Okazawa: okazawa-tky@umin.ac.jp

Abbreviations used in this paper: AMA, α-amanitin; CDDP, cisplatin; FL-YAP, full-length YAP; HD, Huntington's disease; Pol II, polymerase II; polyQ, polyglutamine; siRNA, short inhibitory RNA; TRIAD, transcriptional repression-induced atypical death; YAP, yes-associated protein.

The online version of this article contains supplemental material.

The Journal of Cell Biology, Vol. 172, No. 4, February 13, 2006 589–604
http://www.jcb.org/cgi/doi/10.1083/jcb.200509132

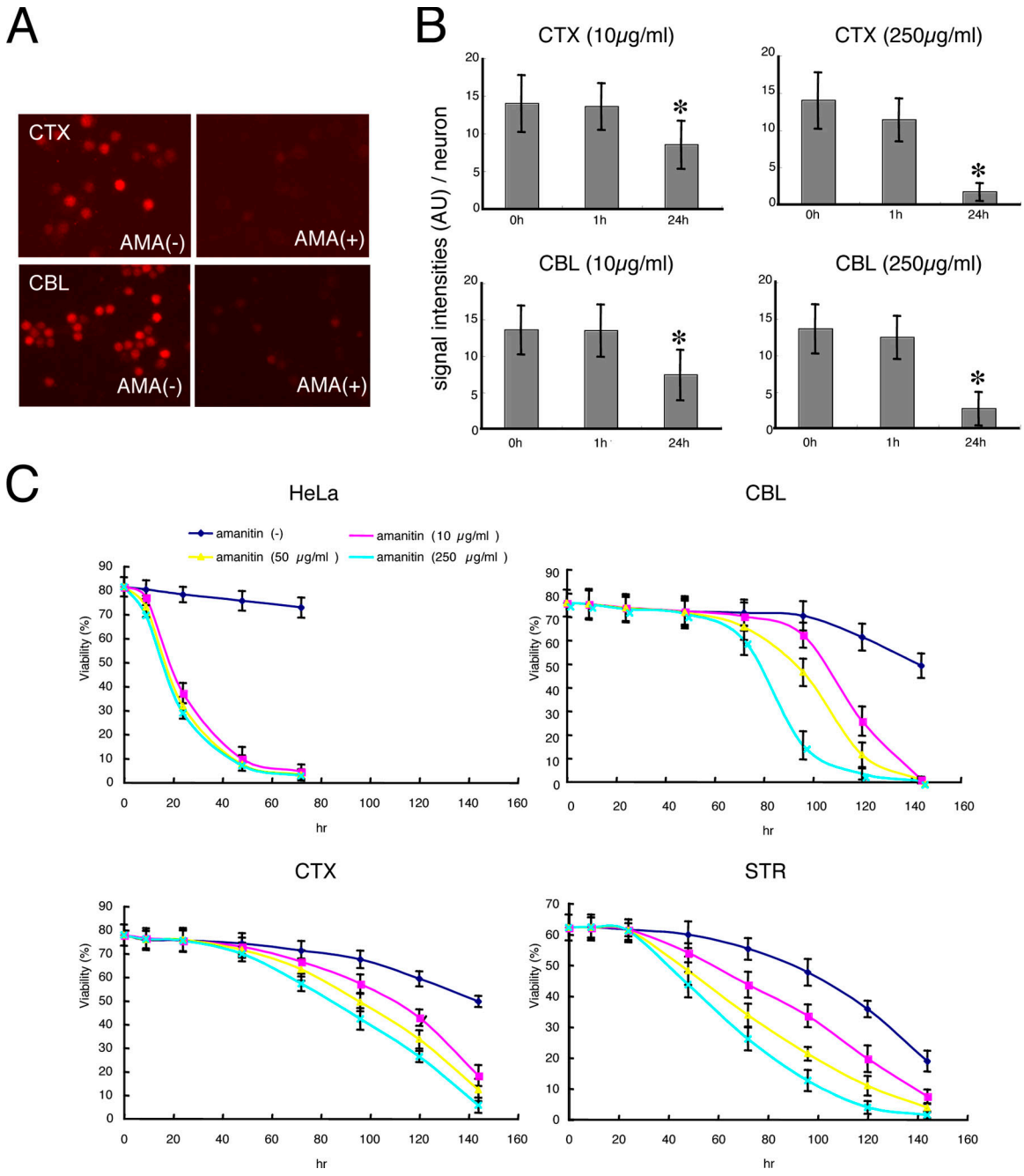

Figure 1. **Transcriptional repression by α-AMA induces a slowly progressive death of primary neurons.** (A) Uptake of BrdU in primary cortical (CTX) or cerebellar (CBL) neurons (Hoshino et al., 2004) was remarkably reduced at 6 h after the addition of 25 μg/ml AMA, indicating that AMA reduces transcription. (B) BrdU uptakes per neuronal nucleus at different concentrations of AMA (10 and 250 μg/ml) were analyzed chronologically. Signal intensities (AU, arbitrary unit) calculated with AQUACOSMOS (Hamamatsu) were obtained from >500 cells. Means ± SD are shown (error bars). Asterisks indicate significant reductions compared with 0 h ($P < 0.01$, *t* test). (C) Survival curves of HeLa cells and primary neurons (cortical, cerebellar, and striatal [STR] neurons) with AMA (10, 25, and 250 μg/ml). Viability (percent) indicates live cells/total cells by trypan blue assay (Tagawa et al., 2004) in six independent wells. Viability was shown as means ± SD of nonstained cells. Viability of HeLa cells declined at 24 h. In primary neurons, a significant reduction was first observed at 72 h at all concentrations of AMA. Of the three types of neuron tested, striatal neurons were the most vulnerable to AMA treatment for 48 h at 25 and 250 μg/ml AMA. $P < 0.05$ (*t* test).

polyQ peptides survives even in affected regions of the brain until the time of necropsy. So far, there is no model that fully explains the lengthy period of cell death in neurodegeneration.

In addition to ER and mitochondrial stresses, transcriptional dysfunction is suggested as a critical pathological component of polyQ diseases (for reviews see Gusella and MacDonald, 2000; Zoghbi and Orr, 2000; Ross, 2002; Taylor et al., 2002; Bates, 2003). Translocation of mutant proteins to the nucleus seems essential for neuronal dysfunction or cell death in polyQ diseases (Klement et al., 1998; Saudou et al., 1998; Katsuno et al., 2003). Numerous transcription-related factors, including LANP, PQBP-1, N-CoR, ARA24, p53, mSin3A, ETO/MTG8,

P160/GRIP1, A2BP1, $TAF_{II}130$, CA150, CRX, Sp1, CtBP, PML, $TAF_{II}30$, NF-κB, and SC35, are known to interact or colocalize with mutant polyQ disease proteins (for reviews see Okazawa, 2003; Sugars and Rubinsztein, 2003). Interaction with polyQ proteins may impair physiological functions of these transcription factors (Okazawa, 2003; Sugars and Rubinsztein, 2003), and, finally, even the general transcription level could be repressed (Hoshino et al., 2004). Some of these polyQ pathology-mediating factors bind directly to the core of transcription machinery, RNA polymerase II (Pol II; Okazawa et al. 2002). Therefore, one of the paramount issues in the field of polyQ diseases is the relationship between transcriptional dysfunction and neuronal death. However, as yet, the role of transcriptional disruption in neuronal death is unclear, as is the mode of neuronal death when transcription is severely impaired.

In this study, we found that inhibition of Pol II–dependent transcription leads neurons to undergo a slowly progressive atypical cell death (transcriptional repression-induced atypical death [TRIAD]) distinct from apoptosis, necrosis, or autophagy in morphological and biochemical analyses. Transcriptome analysis of TRIAD suggested that yes-associated protein (YAP), a known transcriptional cofactor, might be relevant to the death process. YAP, which was originally found as a binding protein to Src homology domain 3 of the yes proto-oncogene product (for review see Sudol et al., 1995), acts as a transcriptional cofactor of p73, mediates the expression of cell death–promoting genes, and induces apoptosis (Yagi et al., 1999; Basu et al., 2003; Melino et al., 2004). We found that in TRIAD, full-length YAP (FL-YAP) is down-regulated, and novel neuron-specific YAPΔC isoforms lacking the cell death–promoting activity sustain to protect neurons in a dominant-negative manner. The shift of balance in YAP isoforms seemed to slow down the cell death signaling pathway of p73 activated by α-amanitin (AMA), at least partially. We further questioned the relevance of YAP and p73 to Huntington's disease (HD) by using cellular, *Drosophila melanogaster*, and mouse models as well as human brain samples. Our data suggest that these molecules might be involved in neuronal death triggered by mutant Htt, the causative gene product of HD.

Results

Transcriptional repression induces an atypical slow neuronal death

To address the role of transcriptional disruption in neuronal death, we first made multiple short inhibitory RNAs (siRNAs) against RNA Pol II to suppress Pol II–dependent transcription. However, suppression of Pol II was inadequate and reminiscent of recent efforts to suppress basic transcription machinery by similar approaches (Ni et al., 2004). Therefore, we used a specific inhibitor of Pol II (AMA) whose three-dimensional molecular structure is exactly complementary to the groove of Pol II, through which mRNA is elongated (Cramer et al., 2001; Bushnell et al. 2002). Different concentrations of AMA were added to the culture medium of HeLa cells, primary rat embryonic (embryonic day [E] 15) cortical neurons, rat E15 striatal neurons, and rat pup cerebellar neurons (postnatal day [P] 7). BrdU up-take assay (Hoshino et al., 2004) showed significant repression of transcription at 6 h of AMA treatment in primary neurons (Fig. 1, A and B) and HeLa cells (not depicted). The survival of AMA-treated cells estimated by trypan blue assay (Fig. 1 C) revealed that AMA induces a slowly progressive cell death in a dose-dependent fashion. This was most pronounced in primary neurons, with half-lives of nearly 5 d. AMA-induced neuronal death was much slower than low potassium–induced apoptosis of cerebellar neurons, whose half-life was ∼12 h (not depicted). The slow progression of AMA-induced neuronal death was confirmed independently by MTT (3-[4, 5-dimethylthiazol-2-yl]-2, 5-diphenyltetrazolium bromide) assay (Fig. S1, available at http://www.jcb.org/cgi/content/full/jcb.200509132/DC1).

A population of HeLa cells (10–30%) began to show cytoplasmic vacuoles proximal to the nucleus (Fig. 2 A, HeLa-TRIAD) from 6–12 h after the addition of AMA. Similar vacuoles were also observed in cortical neurons treated with AMA for 2 d (Fig. 2 A, CTX neuron-TRIAD), although with a diminished frequency (1–5%). It is important to note that the vacuoles did not possess double-membrane structures reminiscent of autophagosomes. No classic apoptotic features such as chromatin condensation, nuclear fragmentation, or apoptotic bodies (Okazawa et al., 1996) were found in these neurons by electron microscopic analysis (Fig. 2 A). In addition, no necrotic features such as mitochondrial dilatation (Fig. 2 A, CTX neuron necrosis) or cytoplasmic ballooning and rupture (Fig. 2 A, CTX neuron necrosis) were observed in primary neurons under TRIAD.

Immunohistochemical analyses using organelle-specific antibodies excluded the idea that the cytoplasmic vacuole was derived from the Golgi apparatus, endosome, lysosome, and mitochondria (Fig. S2, available at http://www.jcb.org/cgi/content/full/jcb.200509132/DC1). Autophagosomes induced by rapamycin and labeled with EGFP-LC3, a marker protein of the autophagosome (Fig. 2 B, top and middle), failed to colocalize with AMA-induced vacuoles (Fig. 2 B, bottom). In addition, the size of AMA-induced vacuoles was larger than that of autophagosomes (Fig. 2 B, bottom). EGFP-LC3 actually expresses the LC3 peptide (Fig. 2 C, arrow), verifying the morphological result. Note that the immunoblot shows a nonspecific band that is consistently detected by this antibody (Fig. 2 C, asterisk; unpublished data). Furthermore, the addition of rapamycin to the medium increased LC3-positive vacuoles but did not affect the formation of LC3-negative vacuoles induced by AMA (Fig. S3 A). Collectively, these data suggested that AMA-induced cell death is distinct from autophagy. Finally, we found colocalization of the vacuoles with ECFP-ER fusion constructs (expressing calreticulin ER-targeting sequences and KDEL ER retrieval tags at the 5′ and 3′ ends, respectively, of ECFP; Fig. 2 D). It suggested that vacuoles might be derived from expanded ER.

In agreement with the absence of morphological features of apoptosis, genomic DNA analyses of cell lines and primary neurons did not show ladder formation after AMA treatment (Fig. 3 A). Caspase-3, -7, and -12 were not remarkably activated in primary neurons by AMA (Fig. 3 B). AMA induced neither the release of cytochrome c into the cytosol from these neurons (Fig. 3 C) nor the interaction of annexin-V with the membrane of these neurons at an early stage (Fig. S3 B). Caspase inhibitors

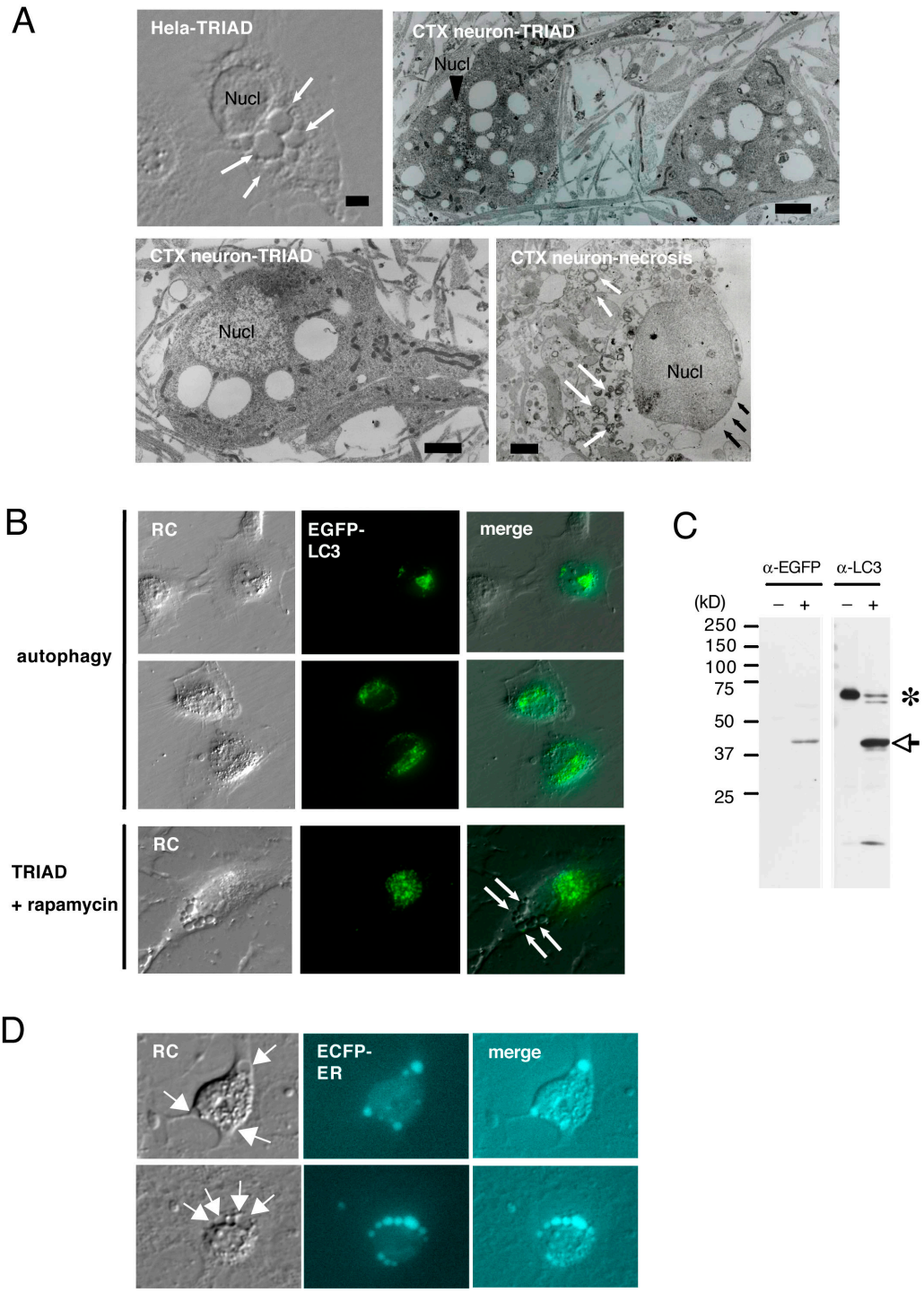

Figure 2. **Morphological features of TRIAD are distinct from those of apoptosis, necrosis, and autophagy.** (A) 10–30% of HeLa cells treated with 25 μg/ml AMA for 24 h (HeLa-TRIAD) showed cytoplasmic vacuoles (white arrows) proximal to the nucleus (Nucl). Electron microscopic analysis of cortical neurons treated with 25 μg/ml AMA for 48 h (CTX neuron TRIAD) revealed similar cytoplasmic vacuoles. Absence of chromatin condensation or nuclear fragmentation distinguishes TRIAD from classical apoptosis. The normal cytoplasm or mitochondria also excludes typical necrosis (bottom left). Electron microscopic analysis of primary cortical neurons in necrosis after freeze-thaw treatment (CTX neuron necrosis) showed the dilation of mitochondria (white arrows) and the rupture of cytoplasm (black arrows). Bars, 1 μm. (B) HeLa cells treated with 200 ng/μl rapamycin for 2 h showed autophagy (top and middle). AMA-induced vacuoles (arrows) did not merge with EGFP-LC3–labeled autophagosomes (bottom). RC, relief contrast. (C) Western blots to verify that pEGFP-LC3 expresses the LC3 peptide. Both anti-EGFP and anti-LC3 antibodies detect EGFP-LC3 (arrow), confirming that the EGFP-LC3 fusion protein is properly expressed. Asterisk indicates a nonspecific band. (D) A marker protein of ER, ECFP-ER (blue), was localized to AMA-induced vacuoles (arrows), suggesting that the vacuoles originate from the ER.

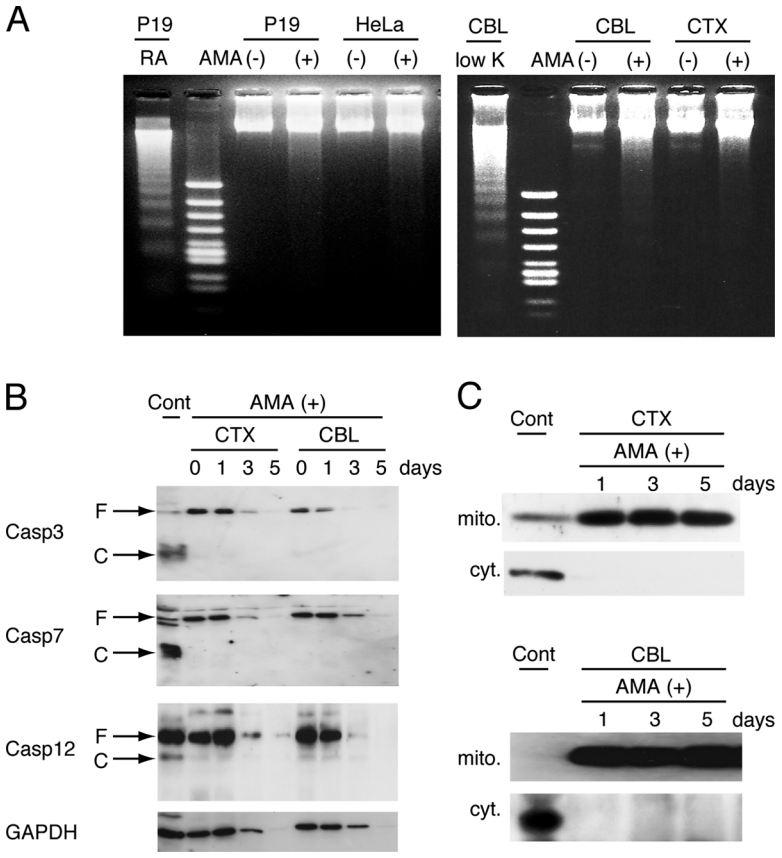

Figure 3. **Biochemical features of TRIAD are distinct from those of apoptosis.** (A) No significant fragmentation of genomic DNA was observed in TRIAD of P19 cells, HeLa cells, primary cerebellar neurons (CBL), and primary cortical neurons (CTX). Genomic DNA was prepared from total (attached and floating) cells cultured with 50 μg/ml AMA for 5 d. As controls of apoptosis, genomic DNA from P19 cells treated with 0.5 μM retinoic acid for 2 d or from cerebellar neurons cultured in a low potassium condition for 2 d were used. RA, retinoic acid. (B) Caspase-3, -7, and -12 were not remarkably activated in cortical and cerebellar neurons treated with 50 μg/ml AMA. Western blots were performed with antibodies specific for each caspase. F and C, full-length and cleaved forms, respectively. (C) No cytochrome c release in cytosol was observed in primary neurons treated with AMA. Mitochondrial (mito) and cytosol (cyt) fractions were prepared from primary cortical or cerebellar neurons treated with 50 μg/ml AMA for 1–5 d and blotted with anticytochrome c antibody.

z-DEVD-fmk and z-VAD-fmk did not repress AMA-induced cell death in neurons or in HeLa cells (not depicted). As expected, cycloheximide did not affect the cell death (not depicted). Calpain inhibitors, including ALLN and ALL, showed no remarkable effect on cell death. Pretreatment of cells with different concentrations of ATP in the medium did not affect AMA-induced cell death (not depicted).

Although AMA is a highly specific inhibitor of Pol II, as confirmed by molecular structural analyses (Cramer et al., 2001; Bushnell et al. 2002), to further verify that AMA-induced cell death is mediated by transcriptional repression, we examined the effect of another type of transcription inhibitor, actinomycin D, on primary neurons (Fig. S4, available at http://www.jcb.org/cgi/content/full/jcb.200509132/DC1). Actinomycin D binds directly to DNA and inhibits transcription (Jones, 1976) by stalling the rapidly moving fraction of Pol II (Kimura et al., 2002). We found that actinomycin D also induced a slowly progressive neuronal death (Fig. S4 A), in which some neurons show cytoplasmic vacuoles similar to those by AMA (Fig. S4 B). Neither DNA fragmentation nor caspase activation was induced by actinomycin D (Fig. S4, C and D). Collectively, our results suggest that AMA induces a slowly progressive TRIAD of neurons that is distinct from apoptosis, necrosis, and autophagy.

Novel YAP isoforms are expressed in neurons specifically

To understand the molecular basis of TRIAD, we conducted microarray analysis and compared gene expression profiles between TRIAD and low potassium–induced apoptosis in primary neurons. To detect initial changes, neurons were harvested at 1 h for RNA preparation. Duplicate experiments allowed us to extract eight genes whose expression levels changed in both apoptosis and TRIAD and a further 11 genes whose expression was changed specifically in TRIAD (Fig. 4 A). The latter group included YAP (Fig. 4 B), a transcriptional coactivator of p73 mediating apoptosis (Basu et al., 2003). Detailed information of the selected genes is provided in Fig. S5 (available at http://www.jcb.org/cgi/content/full/jcb.200509132/DC1). Northern blotting confirmed that AMA treatment down-regulates YAP expression at the level of transcription (Fig. 4 C).

Surprisingly, however, we identified novel isoforms of YAP containing 13-, 25-, and 61-nt inserts (Fig. 4, D and E) in addition to the full-length form by PCR cloning with RNA extracted from nontreated normal cortical and cerebellar neurons. The insert sequences matched genomic sequence with consensus junction sequences (Fig. 5). All three insertions lead to a reading frame shift, causing truncation of the COOH-terminal transcriptional activation domain (Fig. 4, D and E; Yagi et al., 1999). Therefore, we designated them YAPΔCs. Tissue expression profiling by RT-PCR revealed that the 13- and 61-nt insert isoforms (denoted here as Ins13 and Ins61, respectively) relatively specific to neurons (Fig. 4 F). Brain tissue (Fig. 4 F, third lane; not CTX or CBL neurons), including many glial and nonneuronal cells, showed only faint signals of the 13-nt variant comparable with those seen in other tissues (Fig. 4 F). Ins61 was highly specific to cortical neurons (Fig. 4 F). The 25-nt insert could not be detected by RT-PCR. Supporting the expression

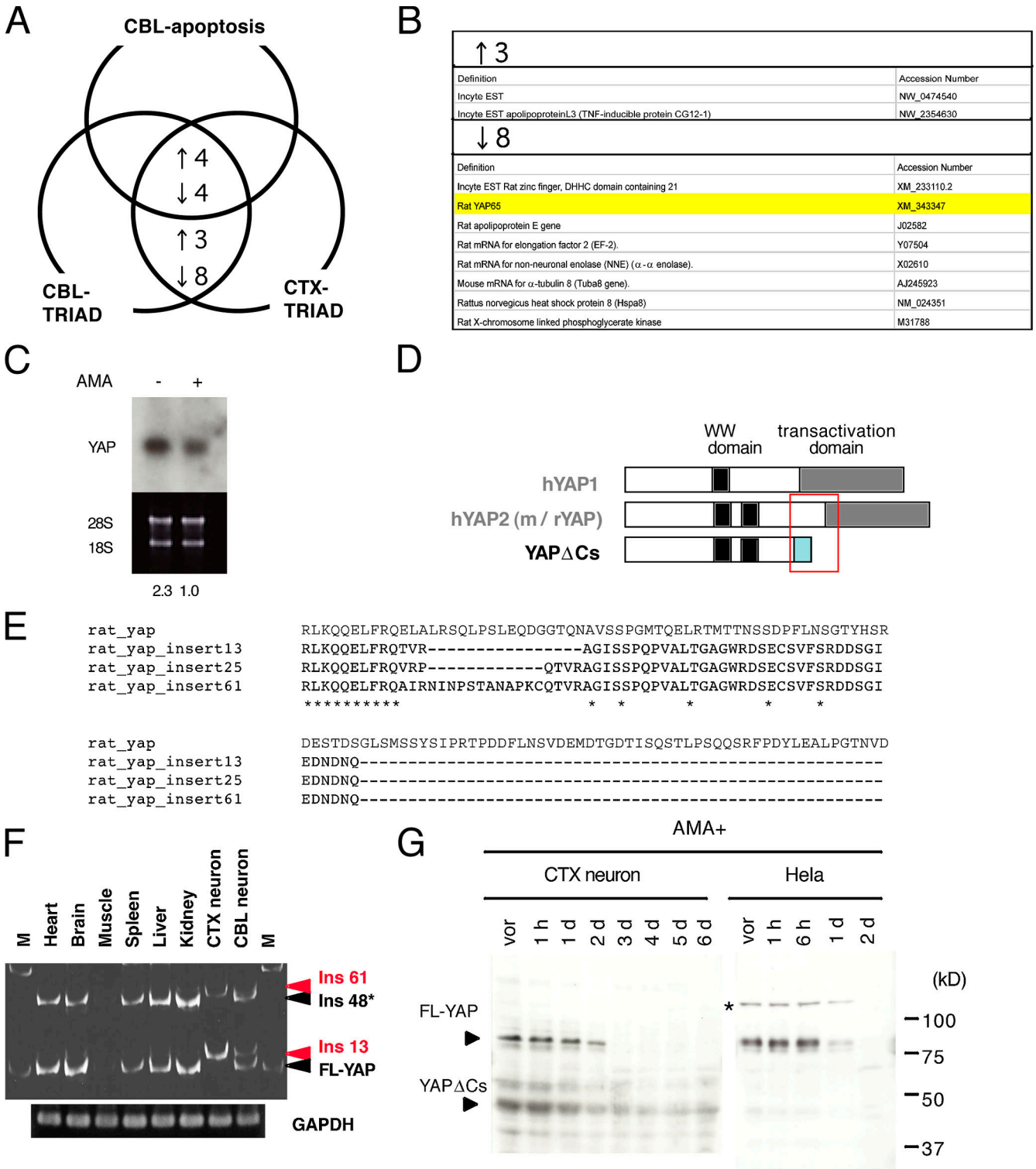

Figure 4. **Molecular features specific to TRIAD include YAP.** (A) Comparison of gene expression profiles among low potassium–induced apoptosis of cerebellar neurons, TRIAD of cerebellar neurons, and TRIAD of cortical neurons. Three genes were up-regulated, and eight genes were down-regulated specifically in TRIAD. (B) Genes specifically changed in TRIAD. (C) Down-regulation of YAP at 1 h after the addition of 25 μg/ml AMA was confirmed by Northern blotting. The bottom numbers indicate the signal intensities of the bands after correction with the 28S controls. (D) PCR cloning of YAP from primary neurons revealed new isoforms lacking the COOH-terminal transactivation domain (YAPΔCs). The scheme shows structures of YAPΔCs, mouse/rat fFL-YAP (m/rYAP = human YAP2), and human YAP1 (hYAP1). (E) Amino acid sequences of YAPΔCs around the junction (boxed area of D). Asterisks indicate conserved amino acids in four isoforms. (F) RT-PCR analysis of tissue-specific expression of YAPΔC isoforms. In addition to YAPΔCs, we detected full-length YAP (FL-YAP) and a previously reported isoform possessing a 48-bp insertion that does not cause a frame shift (ins48). YAPΔCins25 containing a 25-bp insert was not detected in this analysis. M, molecular weight marker. (G) Western blots showing chronological expression of YAP isoforms during TRIAD. In primary cortical neurons (CTX), the expression of YAPΔCs was sustained for 6 d after AMA addition, whereas FL-YAP was repressed within 2 d. Notably, the expression of YAPΔCs was very low in HeLa cells. The asterisk indicates an undetermined band whose expression was correlated with YAP. Vor, before the addition of AMA.

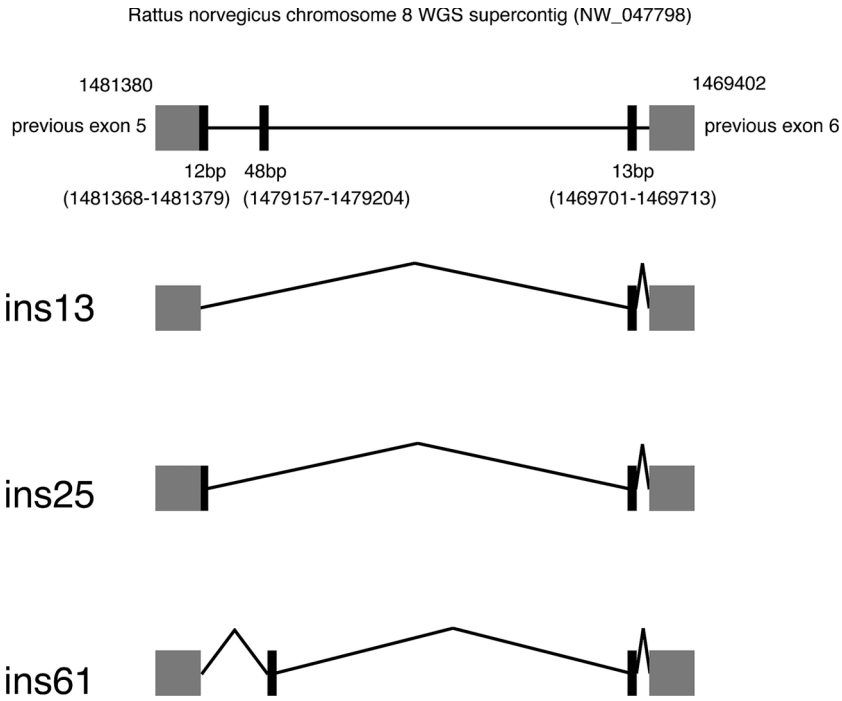

Figure 5. **Genomic structures of YAPΔC isoforms.** Genomic sequence numbers are derived from rat chromosome 8 supercontig. cDNA nucleotide sequences of novel YAP isoforms are available from GenBank/EMBL/DDBJ accession no. DQ186896, DQ186897, and DQ186898. Gray and black boxes are exons; black boxes indicate exons that were newly identified in this study.

of YAPΔCs in neurons, a truncated YAP isoform–specific antibody stained cortical and striatal neurons in immunohistochemistry with human and mouse brains (see Figs. 8 and 9).

In addition, temporal regulation of YAP isoforms during TRIAD was observed by Western blot analysis. Interestingly, although FL-YAP decreased before day 3 in cortical neurons, YAPΔCs were expressed at a relatively constant level (Fig. 4 G). It is also important to note that the levels of YAPΔCs were significantly lower in HeLa cells (Fig. 4 G). These data prompted us to test the function of YAP isoforms in TRIAD.

YAP isoforms modulate TRIAD

p73 and YAP mediate cisplatin (CDDP)-induced apoptosis of a cancer cell line, MCF-7 cells (Basu et al., 2003). In this case, DNA damage induced by CDDP leads to activation of p73, and the transcription cofactor YAP promotes p73-mediated transactivation of cell death genes, including Bax and possibly PUMA (Melino et al., 2004). Truncation of the transcriptional activation domain (Yagi et al., 1999) in YAP may impede transduction of the cell death stimulus, and YAPΔCs may act as dominant negatives against FL-YAP. As expected, luciferase assay showed that expression of YAPΔC isoforms represses p73-mediated activation of the p21/WAF1 gene promoter in MCF-7 cells by CDDP (Fig. 6 A, left; Basu et al., 2003). Overexpression of FL-YAP did not promote transcriptional activation any more (Fig. 6 A) probably because the function of endogenous FL-YAP was saturated. YAPΔCs also showed repressive effects on CDDP-induced apoptosis of MCF-7 cells (Fig. 6 B) mediated by FL-YAP (Basu et al., 2003). In these assays, the expression of each truncate was confirmed in parallel (Fig. 4, A and B; right).

Next, we tested whether YAPΔCs could repress TRIAD of primary cortical neurons (Fig. 6 C). Before the addition of AMA, neurons were infected with adenovirus vectors for YAPΔCs or the empty adenovector (AxCA) as a negative control (Fig. 6 C, left). Expression of YAPΔCs was confirmed by Western blot analysis simultaneously (Fig. 6 C, right). To further test whether YAPΔCs are involved in TRIAD, we transfected a siRNA targeting a sequence shared by three YAPΔC isoforms but not FL-YAP (Fig. 6 D). The siRNA accelerated TRIAD to ~90% (Fig. 6 D), supporting the idea that YAPΔCs suppress the cell death process in TRIAD at least partially.

The suppression of TRIAD by YAPΔCs suggested, in turn, that p73, the target transcription factor of FL-YAP, would be activated in TRIAD. Therefore, we analyzed the amount and phosphorylation of p73 in AMA-treated cortical neurons at day 2. As expected, AMA accelerated the phosphorylation of p73, whereas the total amount of p73 was not changed (Fig. 6 E). Together with the former results, YAPΔCs might inhibit the action of p73, leading neurons to apoptosis by antagonizing FL-YAP, especially at the early phase of TRIAD when FL-YAP is still expressed (Fig. 4 G).

Relevance of YAP isoforms and p73 to HD pathology

To investigate the relevance of YAP isoforms to the HD pathology, we infected primary cortical neurons with adenovirus vectors of YAPΔCs and found that expression of the truncated isoforms repressed Htt111-induced cell death of cortical neurons at 4 d after the infection of adenovirus vectors (Fig. 7 A; Tagawa et al., 2004). Consistently, YAPΔC-specific siRNA promoted Htt-induced cell death of cortical neurons (Fig. 7 B). We also found that mutant Htt induced p73 phosphorylation in cortical neurons at 2 d after infection (Fig. 7 C). Suppression of p73 by siRNA repressed cell death of mutant Htt-expressing neurons at day 4 (Fig. 7 D), suggesting the relevance of p73 to Htt-induced neuronal death. To examine the possible involvement of p73

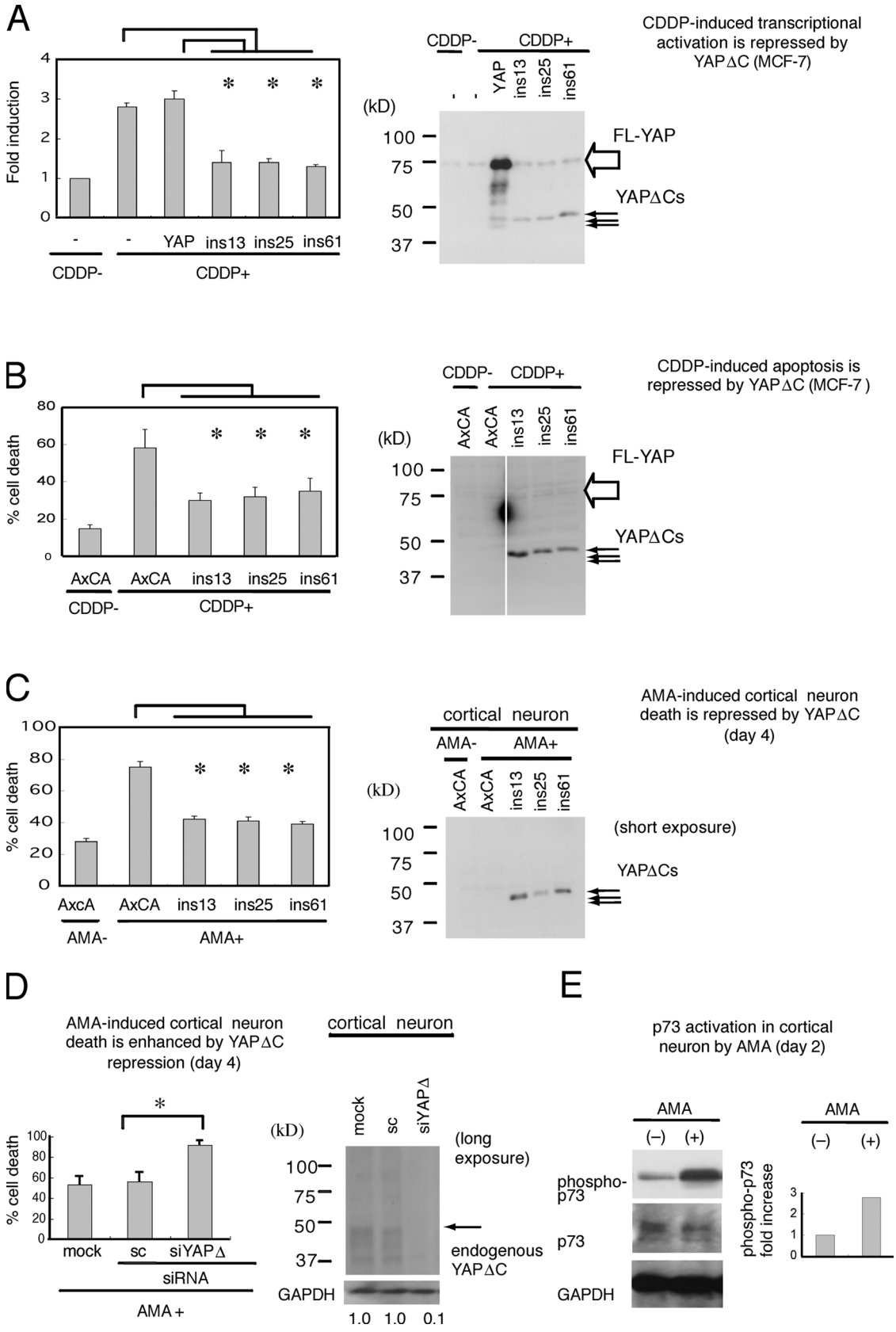

Figure 6. **YAPΔC isoforms repress apoptosis and the TRIAD.** (A) p73-mediated transcriptional activation by cisplatin (CDDP) was repressed by YAPΔCs. Luciferase assays were performed with MCF-7 cells 24 h after transfection of a p21/WAF1 reporter plasmid containing the p73 consensus cis-element and a YAPΔC expression vector (left). 25 μM CDDP was added 2 h after transfection. CDDP increased the transcription level to about threefold. Expression of YAPΔC isoforms (ins13, ins25, and ins61) remarkably repressed transcriptional activation by CDDP. FL-YAP (YAP) did not enhance the transcriptional activation, suggesting that endogenous YAP function was saturated. The expression of YAPs was checked simultaneously (right). $n = 6$. (B) YAPΔCs suppressed

in vivo, we analyzed p73 activation with brain samples of human HD patients. Western blotting with human brain samples suggested higher levels of p73 phosphorylation in HD brains than in control brains (Fig. 7 E).

Correspondingly, immunohistochemical analysis revealed an increase of phosphorylated p73 in striatal neurons of mutant Htt transgenic mice (R6/2) at 4 wk (Fig. 8, middle). It is noteworthy that antiphosphorylated p73 antibody stained both the nucleus and cytoplasm of striatal neurons in R6/2 mice (Fig. 8, middle), although anti-p73 antibody detecting both nonphosphorylated and phosphorylated p73 proteins (full-length and NH_2-terminus deletion forms) dominantly stained the cytoplasm (Fig. 8, left). On the other hand, YAPΔCs were expressed in striatal neurons of both normal and R6/2 transgenic mice, whereas the signal was relatively stronger in transgenic mice (Fig. 8, right).

Furthermore, phosphorylation of p73 was detected in striatal neurons of human HD patients (Fig. 9 A), suggesting that p73 is activated in human HD pathology. In this experiment (Fig. 9 B), because we used the antibody detecting full-length p73 but not ΔNp73, the full-length form of p73 was considered to be phosphorylated (Fig. 9 B, top). YAPΔCs were shown to exist in striatal neurons of human HD patients by a specific antibody (Fig. 9 A, bottom right) and to be colocalized with activated p73 in striatal neurons (Fig. 9 B, bottom). It is important to note that phosphorylated p73 and YAPΔCs were at very low levels in control human brains (Fig. 9 A, top). Collectively, these results suggest the possibility that p73 and YAPΔCs might be involved in the HD pathology.

YAPΔC isoforms attenuate Htt-induced neurodegeneration of *Drosophila*

Finally, we examined the in vivo effect of YAPΔCs on Htt-induced neurodegeneration in *Drosophila* models (Jackson et al., 1998). We generated more than three transgenic fly lines of human YAPΔCs. In the transgenic flies, the expression of YAPΔC protein was triggered by GMR-GAL4 that directs expression in the developing and adult eyes. To analyze the effects on photoreceptor neuron degeneration and/or the characteristic eye phenotype induced by the expression of human Htt120Q, we compared eye phenotypes between the F1 sibling flies at 10 d directly under the microscopy or by toluidine blue staining of 2-μm sections of epon-embedded eye tissues. Ommatidia structure and photoreceptor neurons were severely disrupted in GMR-Htt120Q/GMR-GAL4 double-transgenic flies (BL8533; Jackson et al., 1998), whereas the expression of YAPΔC with a 61-nt insert (YAPΔC61) markedly preserved structure in triple-transgenic flies (GMR-Htt120Q/GMR-GAL4/UAS-YAPΔC61; Fig. 10 A). Expression levels of YAPΔC61 and Htt120Q were checked in the same fly in parallel (Fig. 10 B). Quantitative analysis of rhabdomere numbers per ommatidium in four independent transgenic fly lines supported the repression of neurodegeneration by YAPΔC61 (Fig. 10 C). We observed similar improvement of neurodegeneration in other YAPΔC transgenic *Drosophila* flies (not depicted). Collectively, these in vivo data further suggest the possibility that YAPΔC isoforms might play a protective role against the toxicity of mutant Htt in HD pathology.

Discussion

In this study, we report atypical neuronal death induced by transcriptional repression (TRIAD). Transcriptional repression by Pol II–specific inhibitors leads to a very slow atypical neuronal death whose progression is clearly different from the well-known cell death prototypes. A morphological feature of TRIAD might be the vacuolization of ER, although it should be stressed that the majority of neurons (>90%) do not show remarkable morphological changes. These findings might be relevant to the roles of transcriptional disturbance in HD disease (for review see Gusella and MacDonald, 2000; Zoghbi and Orr, 2000; Ross, 2002; Taylor et al., 2002; Bates, 2003; Okazawa, 2003; Sugars and Rubinsztein, 2003). In addition, the lengthy progression of TRIAD might cast light on the basic question of why neurons stay alive under neurodegeneration for a long period.

To the best of our knowledge, there are a few atypical cell deaths that might be partially analogous to TRIAD. One is a lengthy cell death of *Dictyostelium discoideum* during sorocarp formation, in which dying cells show cytoplasmic vacuolization (Cornillon et al., 1994). The second, termed paraptosis, is induced by the overexpression of the intracellular domain of insulinlike growth factor I (IGF-I) receptor in 293T cells (Sperandio, et al., 2000). Paraptosis is characterized by vacuolization of the ER but no nuclear fragmentation, cellular blebbing, or apoptotic body formation (Sperandio, et al., 2000). These two atypical cell deaths might share molecular pathways (Wyllie and Goldstein, 2001). Although TRIAD shows a related morphological change, TRIAD is clearly different from paraptosis, as the latter is inhibited by both actinomycin D and cycloheximide (Sperandio, et al., 2000). Another point that distinguishes TRIAD from paraptosis is the cell death stimulus. Paraptosis was reported only in ectopic expression of truncated IGF-I receptor in

CDDP-induced apoptosis of MCF-7 cells. 25 μM CDDP was added to the medium 24 h after infection of adenovirus vectors, and cell death assay was performed with annexin-V (Tagawa et al., 2004) in six wells after another 16 h. Adenovirus expression vectors are abbreviated as follows: AxCA, empty adenovirus vector AxCAwt; YAP, AxCAYAP-FL; ins13, AxCAins13; ins25, AxCAins25; and ins61, AxCAins61. Right panel shows the expression of YAP insert forms in cortical neurons. (C) YAPΔCs suppressed TRIAD of cortical neurons. 24 h after infection of adenovirus vectors of YAP isoforms, 25 μg/ml AMA was added. Cell death was assayed with annexin-V (six wells) at 4 d. Right panel shows expression of YAPΔCs in cortical neurons. (D) YAPΔC suppression by siRNA specific to a YAPΔC common sequence (siYAPΔ) enhanced AMA-induced TRIAD of cortical neurons, supporting the idea that YAPΔCs repress TRIAD of cortical neurons. Right panel shows specific repression of YAPΔCs by siYAPΔ. sc, siRNA of a scrambled sequence. 0.5 μg/well siRNA was transfected into cortical neurons (2×10^4 cells/well of 24-well dish), and 25 μM AMA was added to the medium 12 h later. Cell death was quantified by trypan blue staining in six wells at 4 d. (right) Bottom numbers represent relative intensities of the endogenous YAPΔC bands. (A–D) Asterisks indicate significant differences from controls ($P < 0.01$, *t* test). Error bars represent SD. (E) p73 was activated in TRIAD of cortical neurons. Right panel shows fold increase of phosphorylated p73 by AMA treatment (25 μg/ml).

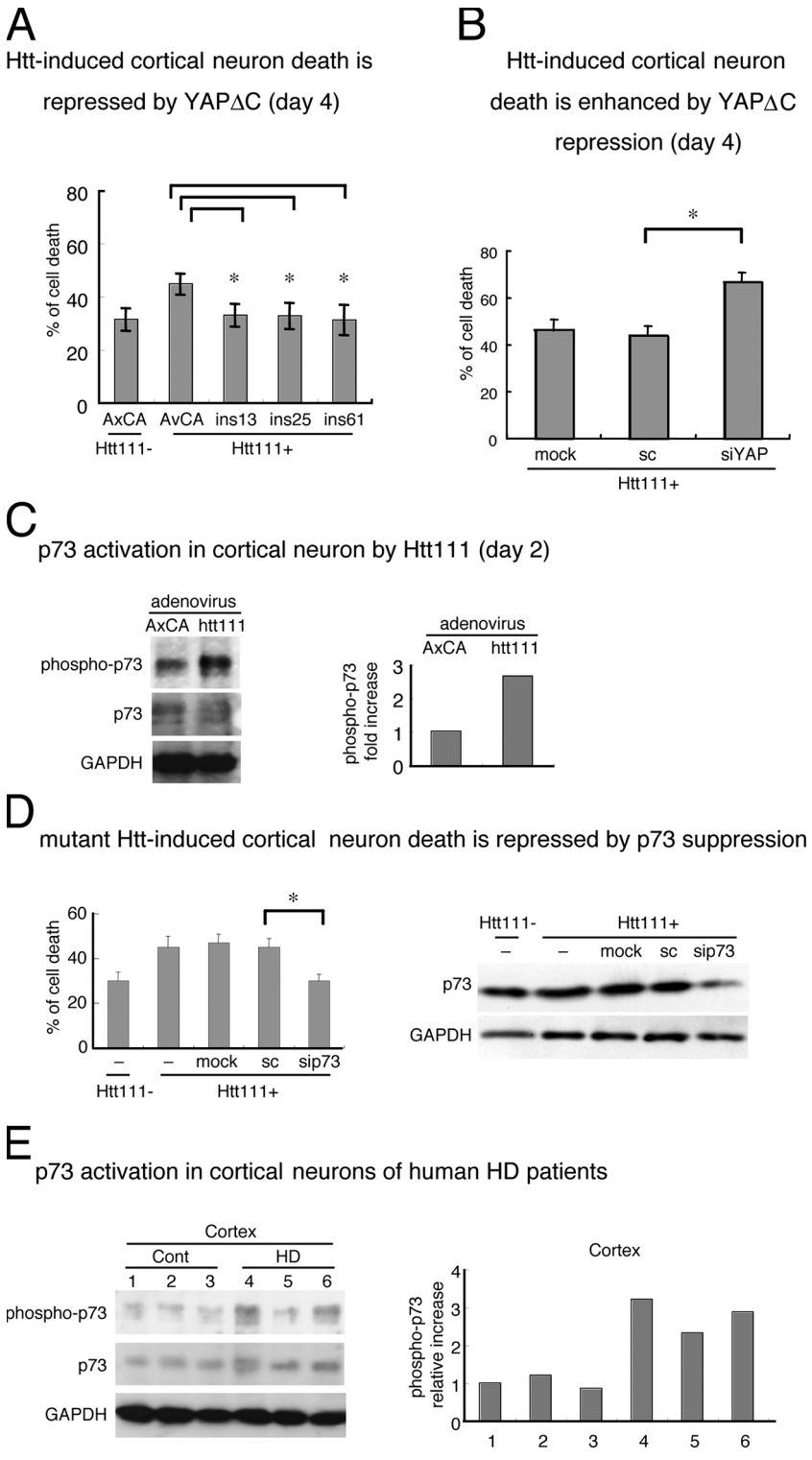

Figure 7. **Relevance of YAPΔC isoforms and p73 to Htt-induced pathology.** (A) YAPΔCs repressed Htt-induced cell death of cortical neurons. Primary cortical neurons were coinfected by adenovirus vectors for mutant Htt (AxCAHtt111) and a YAPΔC (AxCAins13, AxCAins25, or AxCAins61). Cell death was assayed with trypan blue at 4 d. As a control, empty vector (AxCA) was used. Expression of mutant Htt was equivalent among infections (not depicted). (B) Suppression of YAPΔCs by YAPΔC sequence-specific siRNA (siYAPΔ) enhanced mutant Htt-induced cell death of cortical neurons. 0.5 μg/well siRNA was transfected into primary cortical neurons (2×10^4 cells/well of 24-well dish) and infected with adenovirus vectors for mutant *htt* (AxCAHtt111) 12 h later. Cell death was quantified by trypan blue in six wells at 4 d. (C) Phosphorylation of p73 was induced in cortical neurons expressing mutant Htt. Cortical neurons were harvested 48 h after infection of empty adenovirus vector (AxCA) or mutant Htt adenovirus vector (htt111). Immunoblotting was performed with anti-p73, antiphosphorylated p73, or anti-GAPDH (glyceraldehyde-3-phosphate dehydrogenase) antibody (left). Relative values of phosphorylated p73 to total p73 were compared between AxCA-infected and AxCAHtt111-infected neurons (right). (D) Suppression of p73 by siRNA repressed Htt-induced cell death of cortical neurons (left). siRNA transfection and AxCAHtt111 infection were performed similarly to that in B. sip73, siRNA of p73; sc, siRNA of a scrambled sequence; Mock, mock treatment without siRNA. Cell death was quantified by trypan blue staining in four independent wells at 4 d after infection. Right panel shows expression of p73 and GAPDH at the time point of infection of AxCAHtt111 and indicates suppression of p73 by siRNA. (A, B, and D) Asterisks indicate significant reduction of cell death in four independent assays ($P < 0.01$, *t* test). Error bars represent SD. (E) p73 phosphorylation was enhanced in the brain of human HD patients. Cerebral cortex tissues of three HD patients (lanes 4–6) and three controls (lanes 1–3) were analyzed similarly (left). Relative values of phosphorylated p73 to total p73 were calculated (right).

nonneuronal cells (Sperandio, et al., 2000). Furthermore, the role that we find for YAP in TRIAD has not been demonstrated in paraptosis or *D. discoideum* cell death. It is noteworthy that Degterev et al. (2005) has recently reported a new type of cell death—necroptosis. They showed that in the absence of intracellular apoptotic signaling, extrinsic TNF stimulation triggers nonapoptotic cell death, showing necrotic morphology and autophagy. Although rapamycin did not increase typical LC3-negative vacuoles of TRIAD (Fig. S3) negating the autophagic component in TRIAD, we need to analyze carefully the relationship between TRIAD and necroptosis, including the viewpoint of cell death speed.

It is also necessary to consider TRIAD with previous classifications of cell death. Schweichel and Merker (1973) classified three types of cell death. Type 1 was manifested as nuclear condensation and pyknosis, reduced cytoplasmic volume, and

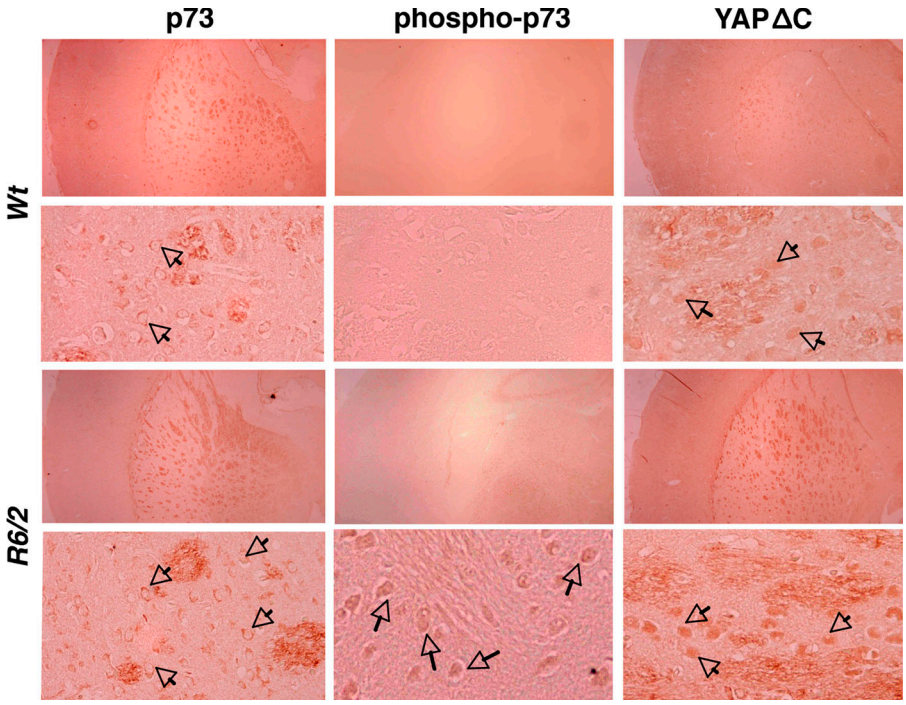

Figure 8. **YAPΔC and phosphorylated p73 are expressed in striatal neurons of Htt transgenic mice.** Immunohistochemical analyses of mutant Htt transgenic (R6/2) and sibling control mice were performed at 4 wk with anti-p73 (full-length form), antiphosphorylated p73, or anti-YAPΔC antibodies. Arrows indicate immunoreactive striatal neurons. Expression of phosphorylated p73 was increased in R6/2 transgenic mice (middle), whereas the total amount of p73 was similar in transgenic and control mice (left). Immunoreactivities of YAPΔC were slightly increased in transgenic mice (right).

late cell fragmentation/phagocytosis. Type 2 was an autophagic vacuolization in the cytoplasm, and type 3 was described as cytoplasmic cell death in which general organelle breakdown was apparent. Type 1 is apoptosis, and types 2 and 3 were necrotic (Schweichel and Merker, 1973). In 1990, Peter Clarke redefined an earlier model of cell death developed by Schweichel and Merker (Clarke, 1990). Clarke's modification was to expand the forms of cytoplasmic cell death into types 3A and 3B. 3A is a nonlysosomal breakdown, and 3B is cytoplasmic (Clarke, 1990). Cells undergoing the 3A type of cell death show an initial swelling of cytoplasmic organelles and the generation of vacuoles that eventually fuse with the extracellular space. A breakup of cell structure without autophagic or heterophagic activity occurs. In type 3B death, which is also known as the cytoplasmic form of cell death, swollen organelles (dilated perinuclear space, ER, and Golgi apparatus) are apparent as well as vacuoles. The cell membrane retracts, and the nucleus becomes karyolytic/edematous. Heterophagic elimination can occur. Type 3B has also been termed paraptosis/oncosis. Among these, TRIAD is close to type 3B. However, in addition to the aforementioned reason, TRIAD seems to be different from type 3B because vacuolization of ER is far more remarkable than morphological changes of other organelles in TRIAD.

In HD models, several studies have reported atypical cell death with cytoplasmic vacuolization. Sapp et al. (1997) reported that mutant Htt accumulates in punctate structures mimicking endosomal–lysosomal organelles of affected HD neurons. They further showed by extensive analyses, including immunoelectron microscopy, that mutant Htt appears in autophagosomes (Kegel et al., 2000). Other studies also pointed out the possible involvement of autophagy in the HD disease pathology (Nagata et al., 2004; Ravikumar et al., 2004; Iwata et al., 2005). Meanwhile, Hirabayashi et al. (2001) isolated VCP (valosin-containing protein)/p97, a member of the AAA+ family of ATPase proteins, as a HD-interacting protein. The expression of the mutant form of VCP leads to cytoplasmic vacuolization, which might be homologous to vacuoles in TRIAD because they were fused to ER (Hirabayashi et al., 2001). Collectively, although our results so far seem to negate the identity of the TRIAD vacuoles to autophagosomes, we cannot exclude the possibility that they might share certain characteristics with the vacuoles reported in HD models.

As for the molecular pathway of TRIAD, YAPΔCs and p73 might modify the process. Up- or down-regulation of YAPΔCs suppresses or enhances TRIAD in cortical neurons, respectively (Fig. 6, C and D). Together with evidence that AMA treatment increases active p73 in neurons (Fig. 6 E) and that YAPΔCs remain during TRIAD of cortical neurons (Fig. 4 G), these data suggest that p73-mediated cell death signaling might be attenuated by YAPΔCs in TRIAD. Consistently, the percentage of morphologically changed neurons (vacuole-possessing neurons) was very low. It might be a reason why TRIAD does not progress rapidly like apoptosis.

p73 was activated in human and mouse HD pathology in vivo (Figs. 8 and 9). YAPΔC isoforms were coexpressed in affected neurons of human HD patients (Fig. 9). Repression of p73 and expression of YAPΔCs attenuated Htt-induced neuronal cell death of primary neurons (Fig. 7, A and D), whereas YAPΔC repression enhanced the neuronal cell death (Fig. 7 B). Furthermore, YAPΔC isoforms suppressed neurodegeneration of photoreceptor cells of *Drosophila* in vivo (Fig. 10). These findings suggest that YAPΔCs and p73 might be relevant to the HD pathology.

p53 has been implicated in the HD pathology because p53 coaggregates with mutant Htt (Steffan et al., 2000). Bae et al. (2005) recently reported that mutant Htt interacts with,

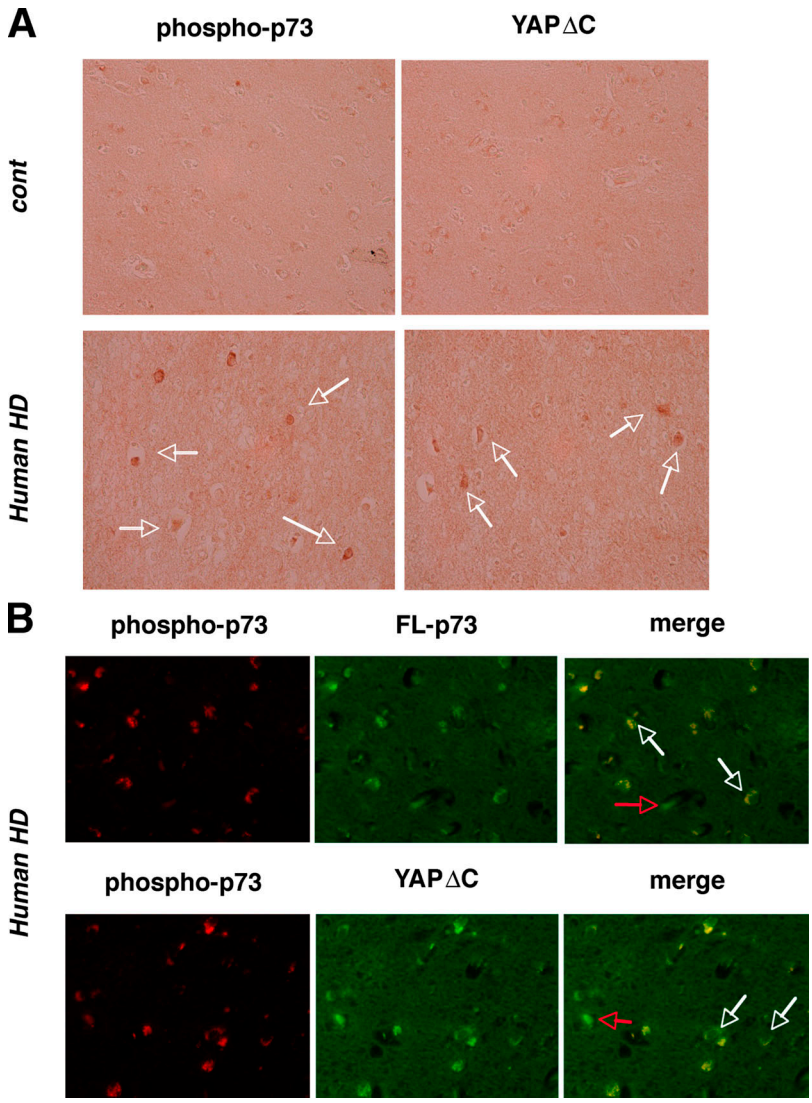

Figure 9. **YAPΔC and phosphorylated p73 are coexpressed in striatal neurons of human HD brain.** (A) Immunoreactivities of phosphorylated p73 and YAPΔC isoforms were increased in striatal neurons of HD patients (arrows). Postmortem brain tissues, including the caudate nucleus, were prepared from three HD patients and three controls. (B) Double staining with anti-p73 rabbit polyclonal antibody specific for full-length p73 but not reactive to ΔNp73 (H-79; 1:500; Santa Cruz Biotechnology, Inc.) and with antiphospho-p73 rabbit polyclonal antibody (1:500; Cell Signaling) showed colocalization of the two signals in most striatal neurons of HD patients (top, white arrows). It suggests that the full-length p73 is phosphorylated in striatal neurons. Bottom panels show that YAPΔC isoforms were colocalized with phosphorylated p73 in striatal neurons (bottom, white arrows). However, a minor portion of neurons expresses only p73 (red arrows).

translocates, and activates p53. They also showed that mating mutant Htt transgenic mice with p53-null mice ameliorates neurological symptoms by mutant Htt (Bae et al., 2005). These results suggest that p53 activation promotes the HD pathology. Because p73 and p53 belong to the same family of transcription factors recognizing a similar consensus sequence on genomic DNA (for review see Irwin and Miller, 2004), the common cascade shared by the two factors should be investigated in the HD pathology. For instance, upstream signals activating these two factors and target gene activation by these transcription factors in the HD pathology should be analyzed in the future. On the other hand, because p53 is suggested to have a direct effect on mitochondria (Mihara et al., 2003), it might be necessary to test whether p73 also plays a similar role.

It is important to note that hyperactive p73 could trigger vacuolar changes of ER in nonneuronal cells (Terrinoni et al., 2004). If this is true, the vacuole formation in TRIAD might be triggered by activated p73. In this case, although ER stress could be induced by mutant polyQ protein (Kouroku et al., 2002; Nishitoh et al., 2002), ER stress might also be evoked by a signal from the nucleus in parallel. Investigation on the possible connection between the nucleus and ER might contribute to understanding the polyQ pathology. The hypothetical pathway should be examined and elucidated in the future. In summary, our results present a novel model of cell death that might cast more light on the HD pathology.

Materials and methods

Primary neuron culture

Cerebral cortex tissues isolated from E17 Wistar rat embryos and cerebellar tissues isolated from P7 Wistar rat pups were minced (with razors) and treated with 0.25% trypsin (Invitrogen) in PBS, pH 7.5, at 37°C for 20 min with gentle shaking every 5 min. After stopping the reaction with DME containing 50% FBS, DNase I (Boehringer) was added to the solution at a final concentration of 100 μg/ml, and tissues dissociated gently by pipetting with blue tips. Cells filtered by nylon mesh (pore size of 70 mm; Falcon; BD Biosciences) were collected by centrifugation, resuspended in DME supplemented with 20 mM glucose, 16 mM sodium bicarbonate, 4 mM glutamine, 25 μg/ml gentamicin, and 10% FBS, and plated on 24-well dishes (Corning) coated by poly-L-lysine (Sigma-Aldrich) at 3×10^5 cells/well. 12 h after plating, cytosine arabinoside was added to the culture medium at 4 M of final concentration to prevent the growth of glial cells. Cerebellar neurons were cultured at high potassium (25 mM) ordinarily but were cultured at 5.4 mM potassium to induce apoptosis. Cortical neurons were cultured at low potassium condition (5.4 mM). Necrosis of cortical neurons

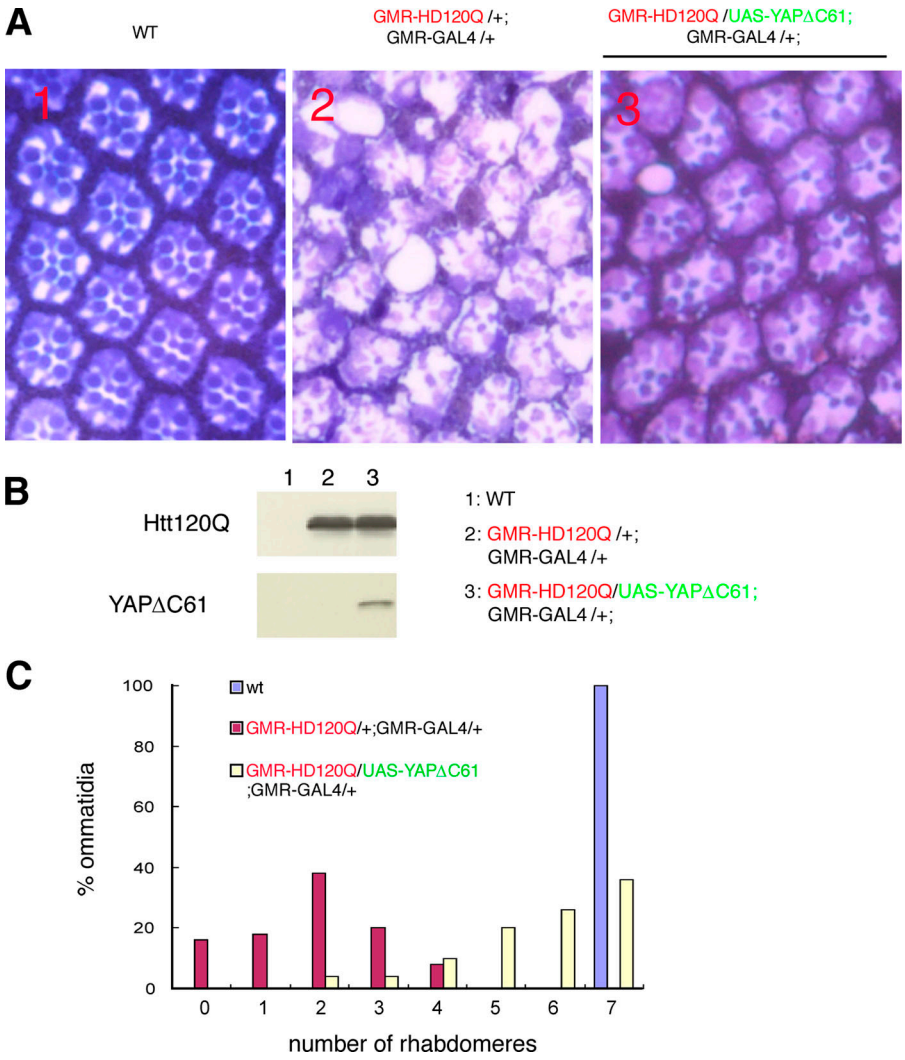

Figure 10. **YAPΔC represses neurodegeneration of *Drosophila* ommatidia.** (A) Morphological analyses of photoreceptor cells in cross sections of *Drosophila* ommatidia. In wild type (WT), a single ommatidium possesses seven rhabdomeres aligned regularly, whereas ommatidia structure and photoreceptor neurons were severely destructed in Htt120Q transgenic flies (GMR-HD120Q/+;GMR-GAL4/+). Expression of YAPins61 remarkably improved the structural anomalies (GMR-HD120Q/UAS-YAΔ61;GMR-GAL4/+). (B) Expression levels of Htt120Q and YAPΔC61 were examined by Western blot analysis in the same fly as shown in Fig. 7 A. (C) Quantitative analysis of rhabdomere numbers per ommatidium in WT, Htt120Q transgenic flies (GMR-HD120Q/+; GMR-GAL4/+), and a representative line of transgenic flies (GMR-HD120Q/UAS-YAPΔ61;GMR-GAL4/+) supported the repression of neurodegeneration by YAPΔC61. More than 30 ommatidia were analyzed in three flies from a line. The results with other three lines of transgenic flies (GMR-HD120Q/UAS-YAPΔ61;GMR-GAL4/+) were basically similar (not depicted).

was induced by the freeze and thaw treatment. To induce TRIAD, AMA (Sigma-Aldrich) was added to the medium at a final concentration of 10 or 25 μg/ml, except for dose–response survival experiments in which the final concentration was 10–250 μg/ml. Actinomycin D (Sigma-Aldrich) was added to the medium at 0.1, 0.5, or 2.5 μg/ml.

Cell death assay

Cell death assays were performed either by trypan blue dye exclusion assay or MTT assay as described in each figure legend. For trypan blue assay, cells were incubated for 5 min in 0.4% trypan blue (Invitrogen). Blue-stained (nonviable) and nonstained (viable) cells were counted (at least 2,000 cells for each condition) in 10–20 visual fields randomly selected at 100× from each of three dishes, as described previously (Tagawa et al., 2004). MTT assay was performed with MTT cell proliferation/viability assay (R&D Systems) according to the commercial protocol. At each time point, the value of drug-treated cells was corrected to the value of nontreated cells as 100%.

Acquisition and processing of microscopic images

Regarding electron microscopic observation, cells were washed with PBS three times, fixed in 2.5% glutaraldehyde/0.1 M phosphate buffer, and treated with 1% OsO_4/0.1 M phosphate buffer for 2 h. Fixed cells were dehydrated through a graded ethanol series and embedded in epoxy resin. Ultrathin sections were stained with uranyl acetate and lead citrate and examined with a transmission electron microscope (H-9000; Hitachi) at 24°C (5,000–50,000×). Numerical aperture of the objective lens was 4, and the imaging medium was air. Data acquisition was performed by electron microscope film.

As for immunocytochemistry, stained cells were observed with a microscope (IX-71; Olympus) at RT (20 or 40×; NA 0.40 or 0.60, respectively), and the imaging medium was air. Data acquisition was performed with a camera (C4742-95-12ERG; Hamamatsu), a controller (ORCA-ER; Hamamatsu), and AQUACOSMOS software (Hamamatsu). The fluorochromes will be described in each method.

Analysis of autophagy

24 h after transfection of pEGFP-LC3, HeLa cells were treated with 10 μg/ml AMA and observed by fluorescence microscopy (Fig. 2). To further analyze the relationship between LC3-positive phagosomes and AMA-induced vacuoles, autophagy was induced by 200 ng/μl rapamycin for 2 h (Sigma-Aldrich; for review see Klionsky and Emr, 2000). LC3-positive and -negative vacuoles were counted in the presence or absence of AMA. HeLa cells were transfected with pEGFP-LC3 by SuperFect (QIAGEN), collected 36 h after transfection, and subjected to Western blot analysis. Anti-EGFP polyclonal antibody (BD Living Colors) and anti-LC3 antibody were used at dilutions of 1:1,000 and 1:2,000, respectively. pEGFP-LC3 and anti-LC3 antibody were gifts from T. Yoshimori (National Institute of Genetics, Mishima, Japan) and N. Mizushima (Tokyo Metropolitan Institute for Medical Science, Tokyo, Japan).

Identification of AMA-induced vacuolization

After treatment of AMA (Sigma-Aldrich) for 6 h, HeLa cells were washed with PBS and fixed using 4% PFA for 15 min at RT. Cells were incubated for 1 h at RT with the following primary antibodies: anti-CCO1 mouse monoclonal antibody (1:100; Invitrogen); anti-EEA1 mouse monoclonal antibody (1:100; Transduction Laboratories); anti-Golgi58k mouse monoclonal antibody (1:100; Sigma-Aldrich); and anti-CD63 (1:100; Cymbus Biotechnology Ltd.). Secondary antibodies conjugated with AlexaFluor488 (Invitrogen) were used at a dilution of 1:1,000 and hybridized for 30 min at RT. HeLa cells were transfected by pEGFP-LC3 (a gift of N. Mizushima and

T. Yoshimori; Kabeya et al., 2000) or pECFP-ER (BD Biosciences) using Superfect (QIAGEN) according to the manufacturer's instructions.

Western blot analyses of caspase-3, -7, and -12

Primary neurons were treated with 25 μg/ml AMA as indicated and were dissolved in 62.5 mM Tris-HCl, pH 6.8, 2% (wt/vol) SDS, 2.5% (vol/vol) 2-mercaptoethanol, 5% (vol/vol) glycerin, and 0.0025% (wt/vol) bromophenol blue on culture dishes. Positive controls for caspase-3 and -7 were prepared from HeLa cells treated with 1 μM staurosporin (Sigma-Aldrich) for 5 h. For a caspase-12 control, HeLa cells were treated with 20 μM A23187 (Calbiochem) for 24 h. Primary and secondary antibodies were diluted as follows: anticaspase-3 polyclonal rabbit antibody (Cell Signaling) at 1:1,000; anticaspase-6 polyclonal antibody (Cell Signaling) at 1:500; anticaspase-7 polyclonal antibody (Cell Signaling) at 1:500; anticaspase-12 polyclonal antibody (14F7; Sigma-Aldrich) at 1:1,000; HRP-conjugated anti–rabbit IgG (GE Healthcare) at 1:3,000; and HRP-conjugated anti–rat IgG (Sigma-Aldrich) at 1:20,000.

Cytochrome c release

10^7 primary cortical neurons were treated with 10 μg/ml AMA as indicated (Fig. 3 C). As a positive control, the same amount of primary cortical neurons were treated with 1 μM staurosporin (Sigma-Aldrich) for 8 h. The cells were washed twice with ice-cold PBS on the dish, collected, and suspended in 500 μl of ice-cold buffer (20 mM Hepes, pH 7.4, 10 mM KCl, 1.5 mM $MgCl_2$, 1 mM EDTA, 1 mM DTT, 1 mM PMSF, and 250 mM sucrose) and disrupted by moderate strokes in a homogenizer. The homogenate was centrifuged twice at 1,300 *g* for 5 min to remove nuclei, unbroken cells, and large membrane fragments. From the supernatant, mitochondria were isolated by further centrifugation at 17,000 *g* and 4°C for 15 min. Pellets were dissolved in the sample buffer described above, separated by 15% SDS-PAGE, blotted to polyvinylidene difluoride membranes (Fine Trap; Nihon Eido), incubated with cytochrome c monoclonal antibody (1:1,000; Santa Cruz Biotechnology, Inc.), and subjected to HRP-coupled detection. The supernatant of the final centrifugation was used as a cytosolic fraction.

RNA probes for microarray analyses

Cells in culture dishes are harvested in TRIzol reagent (Invitrogen) after rinsing with PBS twice, and total RNA was prepared according to the manufacturer's protocol. Labeling and amplification of RNA was performed using the Agilent Fluorescent Linear Amplification Kit (G2554A; Agilent Technologies) according to the manufacturer's protocol. First, double-stranded cDNAs with a T7 promoter were synthesized from 2 μg of total RNA by Moloney murine leukemia virus reverse transcriptase using an oligonucleotide dT-primer, which contains the T7 promoter sequence, and random hexamers (40°C for 4 h). Then, using these double-stranded cDNAs as templates, cRNA was synthesized by T7 RNA polymerase using Cy3- or Cy5-labeled CTP (40°C for 1 h). cRNAs from AMA-treated cortical neurons, AMA-treated cerebellar neurons, or low potassium–exposed cerebellar neurons were labeled with Cy3 or Cy5. Synthesized cRNA was precipitated with lithium chloride, ethanol rinsed, and dissolved in nuclease-free water. To check the quality of cRNA, OD_{260}, OD_{280}, A_{552} (for Cy3), and A_{650} (for Cy5) measurements were taken. Then, OD_{260}/OD_{280}, amplification rates and dye incorporation rates (pmol/μg RNA) of cRNA were calculated. Using these criteria, we found that our samples were of high quality (OD_{260}/OD_{280}, <2.0; amplification rate, <400; Cy3 incorporation, <15 [pmol/μg RNA]; and Cy5 incorporation, <12 [pmol/μg RNA]).

Microarray analysis

Hybridization procedures were performed using the In situ Hybridization Kit Plus (5184–3568; Agilent Technologies) according to the manufacturer's protocol. First, Cy3- and Cy5-labeled cRNAs (1 μg each) were mixed and incubated with fragmentation buffer (Agilent Technologies) at 60°C for 30 min. Mouse Development Oligo Microarray (G4120A; Agilent Technologies), which contains 20,371 60-mer oligonucleotides from mouse cDNA, was hybridized with fragmented cRNA targets at 60°C for 17 h using CHBIO (Hitachi). Hybridized microarrays were rinsed twice and dried by spraying N_2 gas (99.999%) using a filter-equipped air gun (mycrolis KK; Nihon).

Fluorescent signals were read using a microarray scanner (CRBIO IIe; Hitachi). Data were analyzed using analysis software (DNASIS array; Hitachi). In brief, data either from control spots or from spots containing high intensities of artificial signals were removed. Then, the signal intensity of each spot was normalized to equalize total signal intensity. Normalized signal intensity of each spot was plotted on a scatter plot with Cy3 fluorescence on the y axis and Cy5 fluorescence on the x axis. The ratio of Cy3/Cy5 fluorescence was calculated, and genes with outstanding Cy3/Cy5 ratios of >2.0 or <0.5 were listed.

To confirm the results, we also used a rat cDNA microarray (G4105A; Agilent Technologies) on which cDNAs (mean length of 500 bases) derived from 14,811 genes were spotted. cDNA probes were labeled by the Direct Label Kit (G2557A; Agilent Technologies) with an oligonucleotide dT primer according to the manufacturer's protocol. The chips were hybridized at 65°C for 17 h and washed with 0.5× SSC and 0.01% SDS for 5 min at RT and with 0.06× SSC for 2 min at RT.

PCR cloning

RT-PCR cloning of YAP was conducted with cDNA reverse transcribed from 1 mg of total RNA prepared from rat cortical neurons by using the RNA LA PCR Kit (Takara) and primers F (5′-GGAATTCTATGGAGCCCGCGCAA-3′) and R (5′-ACGCGTCGACCTATAACCACGTGAG-3′). PCR amplification was performed for 35 cycles (94°C for 30 s, 52°C for 30 s, and 72°C for 90 s). The resultant cDNAs were subcloned between EcoRI and SalI sites of pBluescriptII SK+. Nucleotide sequences were determined by using M13 or synthesized internal primers and the ABI PRISM BigDye Terminator Cycle Sequencing Kit version 3.1 (Applied Biosystems) and ABI PRISM 310 DNA Sequencer (Applied Biosystems). pBluescript plasmids containing 13-, 25- and 61-nt insert forms of YAP were named pBSins13, pBSins25, and pBSins61, respectively. The cDNA of each YAP insert was subcloned into pCI neo (Promega) and denoted pClins13, pClins25, and pClins61, respectively.

Luciferase assay

5×10^6 cells MCF-7 cells were transiently transfected with 5 μg of pGL3-Bax-Luc (Strano et al., 2002) with pCI–FL-YAP, -YAPΔC (pClins13, pClins25, and pClins61), or control pCI-neo using LipofectAMINE 2000 (Invitrogen) according to the protocol described previously (Basu et al., 2003).

Western blot analysis

Cells were resuspended in 62.5 mM Tris-HCl, pH 6.8, 2% (wt/vol) SDS, 2.5% (vol/vol) 2-mercaptoethanol, 5% (vol/vol) glycerin, and 0.0025% (wt/vol) bromophenol blue on culture dishes. Cell lysates prepared from wells containing either 3.3×10^4 HeLa cells or 1.0×10^5 primary neurons were subject to SDS-PAGE gels, transferred onto polyvinylidene difluoride membranes (Fine Trap; Nihon Eido), incubated with each primary antibody for 1 h and the corresponding HRP-conjugated secondary antibody for 30 min, and visualized using the ECL Western Blotting Detection System (GE Healthcare). The dilution conditions for primary and secondary antibodies were as follows: anti-YAP polyclonal rabbit antibody (H-125; Santa Cruz Biotechnology, Inc.) at 1:1,000; anti-GAPDH mouse monoclonal antibody (Chemicon) at 1:100,000; HRP-conjugated anti–mouse IgG (GE Healthcare) at 1:5,000; and HRP-conjugated anti–rabbit IgG (GE Healthcare) at 1:3,000. Anti-YAPΔC rabbit polyclonal antibody was raised against the common COOH-terminal peptide (SVFSRDDSGIEDNDNQ) by immunizing rabbits and was used for Western blotting at a 1:1,000 dilution.

Adenovirus vector construction

The replication-defective adenovirus vectors were constructed by using the Adenovirus Expression Vector Kit (Takara) according to the manufacturer's instructions. In brief, cDNAs of YAP isoforms were digested with EcoRI and SalI from pBSYAP-FL (containing rat FL-YAP), pBSins13, pBSins25, and pBSins61. Ends were blunted using the blunting high kit (Toyobo), and each insert was subcloned into the SwaI site of the pAxCAwt cosmid (Takara). The resultant cosmids were transfected into 293T cells by the calcium-phosphate method with digested DNA of adenovirus and the medium containing dead cells recovered as the virus solution. After two or three rounds of amplification (5×10^8 and $\sim 5 \times 10^9$ plaque-forming units/ml), clonality was checked by restriction with endonucleases and PCR. We designated the adenovirus vectors AxCAYAP-FL, AxCAins13, AxCAins25, and AxCAins61. The vectors were used for infection of HeLa cells and primary neurons at a multiplicity of infection (MOI) of 100. Preliminary examination of the efficiency of protein expression and toxicity of adenovirus was performed by infecting primary neurons with a vector for EGFP and a mock vector at multiple MOI, respectively. More than 90% of the neurons expressed EGFP at an MOI of 100. The difference in cell death percentage between noninfected and mock-infected neurons estimated by trypan blue staining was $<3\%$ when the MOI did not exceed 500.

Northern blotting

10 μg of total RNA from primary culture neurons was subjected to electrophoresis using a MOPS/formaldehyde gel. Separated RNAs were

capillary blotted to Hybond-N (GE Healthcare) and fixed by UV cross-linking (120,000 μJ/cm^2). Full-length cDNA of ins61 was digested from pB-Sins61, purified from gel, and radiolabeled using α-[^{32}P]dCTP (GE Healthcare) and a random primer DNA labeling kit (Takara). ^{32}P-labeled probes were hybridized to nylon membrane at 60°C overnight with shaking. Hybridized membrane was rinsed with 1× SSC, 0.1% SDS at 50°C for 20 min twice, and with 0.1× SSC and 0.1% SDS at 60°C for 20 min twice. The membrane was then exposed to X-ray film for an appropriate time at −80°C.

RNA interference

Cells were transfected with siRNA oligonucleotides by RNAiFect (QIAGEN) according to the manufacturer's instructions. 2.5 × 10^4 cells in six-well dishes were infected at 0.5 μg siRNA/well 24 h after plating. 24 h after infection, AMA was added to a final concentration of 10 μg/m. The cell death assay was performed after another 24 h. Sequences of siRNAs of YAP and p73 were the same as those published previously (Basu et al., 2003). Sequences of the YAPΔC isoform-specific siRNAs were 5′-r(ACCGTCAGAGCGGGAATTAGCTC)d(TT)-3′ and 5′-r(GAGCTAATTCCCGCTCTGACGGT)d(TT)-3′, corresponding to the common exon among three YAPΔC isoforms.

Analysis of p73 phosphorylation

HeLa cells and cortical neurons were treated with 10 μg/ml AMA for 6 h and 2 d, respectively. For the Htt experiments, HeLa cells and primary cortical neurons were harvested 2 d after infection. HeLa cells or primary cortical neurons were dissolved in TNE buffer (10 mM Tris-HCl, pH 7.8, 1% NP-40, 0.15 M NaCl, 1 mM EDTA, 10 μg/ml aprotinin, 1 mM PMSF, 1 mM Na_3VO_4, and 1 mM NaF), and the supernatant was collected after centrifugation. Nonspecific binding proteins were removed by preincubation with protein G–Sepharose beads (GE Healthcare), and anti-p73 goat polyclonal antibody (S-20; Santa Cruz Biotechnology, Inc.) was added to the supernatant at 1:200. The mixture was incubated overnight at 4°C and precipitated by protein G–Sepharose beads for 1 h at 4°C. After washing five times with TNE, the precipitate was boiled in 2× loading buffer and subjected to Western blot analysis. The filter was blotted with the anti-p73 goat polyclonal antibody (S-20; 1:1,000; Santa Cruz Biotechnology, Inc.) or antiphosphorylated p73 rabbit polyclonal antibodies (1:1,000; Cell Signaling) followed by HRP-coupled detection. For analysis of p73 phosphorylation in human brain, each sample of striatum was homogenized in 20× vol TNE and subjected to the detection of p73 phosphorylation by Western blotting and immunohistochemistry.

Immunohistochemistry of transgenic mouse brains

Brain tissues were prepared from 4-wk-old R6/2 transgenic mice and the littermates. After deparaffinization and rehydration, the sections were incubated sequentially with 3% hydrogen peroxide for 30 min to inhibit endogenous peroxidase, 1.5% normal goat serum in PBS for 1 h at RT, and either a rabbit polyclonal antibody specific for full-length p73 that was raised against the NH_2-terminal 80 amino acids of p73 (H-79; 1:100; Santa Cruz Biotechnology, Inc.), an antiphospho-p73 rabbit polyclonal antibody (1:50; Cell Signaling), or an anti-YAPΔC rabbit polyclonal antibody against the common COOH-terminal peptide (SVFSRDDSGIEDNDNQ) of YAPΔC isoforms (1:100). These incubations were overnight at 4°C. The slides were incubated with anti–rabbit EnVision conjugates of secondary antibody (DakoCytomation) for 1 h at RT and visualized with DAB (Sigma-Aldrich). The same protocol was applied for immunohistochemistry of human brain sections. For double staining, each section after the first staining was agitated in stripping buffer (0.05 M glycine-HCl, pH 3.6) for 3 h at RT, hybridized with anti–glial fibrillary acidic protein polyclonal antibody (1:1,000; Chemicon) overnight at 4°C and with anti–rabbit EnVision conjugates of secondary antibody (DakoCytomation) for 1 h at RT, and visualized with DAB (Sigma-Aldrich) containing $NiCl_2$ $6H_2O$.

Immunohistochemistry of human brain samples

Postmortem brain tissues were prepared from HD patients diagnosed by CAG repeat expansion. The paraffin-embedded section was deparaffinized, rehydrated, and blocked with 5% skim milk in PBS for 30 min at RT. Single staining was performed as described in the previous section. For double staining, the section was incubated with anti-p73 rabbit polyclonal antibody specific for full-length p73 (H-79; 1:500; Santa Cruz Biotechnology, Inc.) or with or an anti-YAPΔC rabbit polyclonal antibody overnight at 4°C, washed with TNT (0.1% Tween 20–TBS) buffer twice, incubated with HRP-conjugated secondary antibody (1:3,000; GE Healthcare) for 1 h at RT, washed with TNT buffer twice, and visualized by incubation with FITC-tyramide (1:200; PerkinElmer) for 10 min. The tyramide complex was stripped off by incubation with 0.05 M glycine-HCl, pH 3.6, for 3 h at RT. After complete stripping, antiphospho-p73 rabbit polyclonal antibody (1:500; Cell Signaling) was hybridized and visualized with Cy3-conjugated secondary antibody (1:1,000; Chemicon).

***Drosophila* genetics**

Fly culture and mating were carried at 25 and 60% humidity. P(GMR-GAL4) (BL8121) and P(GMR-HD120Q) (BL8533) (Jackson et al., 1998) were obtained from the Bloomington Stock Center. The UAS-YAPins13, 25, and 61 transgenic flies were generated by cloning the corresponding human cDNA into pUAST transformation vector and injecting the construct DNA into cantonized w(cs10) (Dura et al., 1993) by standard methods (Rubin and Spradling, 1982). Genotypes of the YAP transgenic flies were determined by mating them with double balancer flies, and they were kept with a balancer gene before use. To analyze the effects of YAPins61 on photoreceptor neuron degeneration and/or the characteristic eye phenotype induced by the expression of human Htt 120Q, we compared eye phenotypes between the F1 sibling flies (GMR-HD120Q/UAS-YAPΔ61;GMR-GAL4/+ vs. GMR-HD120Q/+; GMR-GAL4/+) directly under the microscopy VH5000 (Keyence) or by toluidine blue staining of 2-μm sections of epon-embedded eye tissues.

***Drosophila* histology**

For sections of fly photoreceptor neurons, adult heads (0–10 d) were prefixed overnight in 2% formaldehyde and 2.5% glutaraldehyde in 0.1 M phosphate buffer overnight at 4%, postfixed in 1% osmium at RT for 3 h followed by dehydration in ethanol and embedding in epon for vertical and transversal semi-thin sections (2 μm), and stained with toluidine blue. At least five individuals were examined in each fly line and at each time point.

Online supplemental materials

Fig. S1 shows an MTT assay of TRIAD. Fig. S2 shows immunocytochemical analysis of TRIAD-associated vacuoles. Fig. S3 shows that TRIAD is neither autophagy nor apoptosis. Fig. S4 shows that actinomycin D also induced TRIAD. Fig. S5 shows transcriptome analysis of TRIAD. Online supplemental material is available at http://www.jcb.org/cgi/content/full/jcb.200509132/DC1.

We thank Dr. Andrew H. Wyllie for critical comments and Dr. Kathleen Isacson for naming of the new neuronal death. We thank Dr. Masao Shibata and Ms. Hiroko Ueda for their support in antibody generation and electron microscope analysis, respectively.

This work was supported by grants from the Japan Ministry of Education, Culture, Science, Sports and Technology (16650076); Japan Society for the Promotion of Science (16390249); Japan Science and Technology Agency (Precursory Research for Embryonic Science and Technology); the National Institutes of Health; and the Human Frontier Science Program.

Submitted: 21 September 2005
Accepted: 9 January 2006

References

Bae, B.-I.I., H. Xu, S. Igarashi, M. Fujimoto, N. Agrawal, Y. Taya, S.D. Hayward, T.H. Morgan, C. Montell, C.A. Ross, et al. 2005. p53 mediates cellular dysfunction and behavioral abnormalities in Huntington's disease. *Neuron*. 47:29–41.

Basu, S., N.F. Totty, M.S. Irwin, M. Sudol, and J. Downward. 2003. Akt phosphorylates the Yes-associated protein, YAP, to induce interaction with 14-3-3 and attenuation of p73-mediated apoptosis. *Mol. Cell*. 11:11–23.

Bates, G. 2003. Huntingtin aggregation and toxicity in Huntington's disease. *Lancet*. 361:1642–1644.

Bushnell, D.A., P. Cramer, and R.D. Kornberg. 2002. Structural basis of transcription: alpha-amanitin-RNA polymerase II cocrystal at 2.8 A resolution. *Proc. Natl. Acad. Sci. USA*. 99:1218–1222.

Clarke, P.G. 1990. Developmental cell death: morphological diversity and multiple mechanisms. *Anat. Embryol. (Berl.)*. 181:195–213.

Cramer, P., D.A. Bushnell, and R.D. Kornberg. 2001. Structural basis of transcription: RNA polymerase II at 2.8 angstrom resolution. *Science*. 292:1863–1876.

Cornillon, S., C. Foa, J. Davoust, N. Buonavista, J.D. Gross, and P. Goldstein. 1994. Programmed cell death in *Dictyostelium*. *J. Cell Sci.* 107:2691–2704.

Degterev, A., Z. Huang, M. Boyce, Y. Li, P. Jagtap, N. Mizushima, G.D. Cuny, T.J. Mitchison, M.A. Moskowitz, and J. Yuan. 2005. Chemical inhibitor

of nonapoptotic cell death with therapeutic potential for ischemic brain injury. *Nat. Chem. Biol.* 1:112–119.

Dura, J.M., T. Preat, and T. Tully. 1993. Identification of linotte, a new gene affecting learning and memory in *Drosophila melanogaster*. *J. Neurogenet.* 9:1–14.

Gusella, J.F., and M.E. MacDonald. 2000. Molecular genetics: unmasking polyglutamine triggers in neurodegenerative disease. *Nat. Rev. Neurosci.* 1:109–115.

Hirabayashi, M., K. Inoue, K. Tanaka, K. Nakadate, Y. Ohsawa, Y. Kamei, A.H. Popiel, A. Sinohara, A. Iwamatsu, Y. Kimura, et al. 2001. VCP/p97 in abnormal protein aggregates, cytoplasmic vacuoles, and cell death, phenotypes relevant to neurodegeneration. *Cell Death Differ.* 8:977–984.

Hoshino, M., K. Tagawa, T. Okuda, and H. Okazawa. 2004. General transcriptional repression by polyglutamine disease proteins is not directly linked to the presence of inclusion bodies. *Biochem. Biophys. Res. Commun.* 313:110–116.

Irwin, M.S., and F.D. Miller. 2004. p73: regulator in cancer and neural development. *Cell Death Differ.* 11:S17–S22.

Iwata, A., J.C. Christianson, M. Bucci, L.M. Ellerby, N. Nukina, L.S. Forno, and R.R. Kopito. 2005. Increased susceptibility of cytoplasmic over nuclear polyglutamine aggregates to autophagic degradation. *Proc. Natl. Acad. Sci. USA*. 102:13135–13140.

Jackson, G.R., I. Salecker, X. Dong, X. Yao, N. Arnheim, P.W. Faber, M.E. MacDonald, and S.L. Zipursky. 1998. Polyglutamine-expanded human huntingtin transgenes induce degeneration of *Drosophila* photoreceptor neurons. *Neuron*. 21:633–642.

Jones, G.H. 1976. RNA synthesis in *Streptomyces* antibiotics: in vitro effects of actinomycin and transcriptional inhibitors from 48-h cells. *Biochemistry*. 15:3331–3341.

Kabeya, Y., N. Mizushima, T. Ueno, A. Yamamoto, T. Kirisako, T. Noda, E. Kominami, Y. Ohsumi, and T. Yoshimori. 2000. LC3, a mammalian homologue of yeast Apg8p, is localized in autophagosome membranes after processing. *EMBO J.* 19:5720–5728.

Katsuno, M., H. Adachi, M. Doyu, M. Minamiyama, C. Sang, Y. Kobayashi, A. Inukai, and G. Sobue. 2003. Leuprorelin rescues polyglutamine-dependent phenotypes in a transgenic mouse model of spinal and bulbar muscular atrophy. *Nat. Med.* 9:768–773.

Kegel, K.B., M. Kim, E. Sapp, C. McIntyre, J.G. Castano, N. Aronin, and M. Difiglia. 2000. Huntingtin expression stimulates endosomal-lysosomal activity, endosome tubulation, and autophagy. *J. Neurosci.* 20:7268–7278.

Kimura, H., K. Sugaya, and P.R. Cook. 2002. The transcription cycle of RNA polymerase II in living cells. *J. Cell Biol.* 159:777–782.

Klement, I.A., P.J. Skinner, M.D. Kaytor, H. Yi, S.M. Hersch, H.B. Clark, H.Y. Zoghbi, and H.T. Orr. 1998. Ataxin-1 nuclear localization and aggregation: role in polyglutamine-induced disease in SCA1 transgenic mice. *Cell*. 95:41–53.

Klionsky, D.J., and S.D. Emr. 2000. Autophagy as a regulated pathway of cellular degradation. *Science*. 290:1717–1721.

Kouroku, Y., E. Fujita, A. Jimbo, T. Kikuchi, T. Yamagata, M.Y. Momoi, E. Kominami, K. Kuida, K. Sakamaki, S. Yonehara, et al. 2002. Polyglutamine aggregates stimulate ER stress signals and caspase-12 activation. *Hum. Mol. Genet.* 11:1505–1515.

Melino, G., F. Bernassola, M. Ranalli, K. Yee, W.X. Zong, M. Corazzari, R.A. Knight, D.R. Green, C. Thompson, and K.H. Vousden. 2004. p73 Induces apoptosis via PUMA transactivation and Bax mitochondrial translocation. *J. Biol. Chem.* 279:8076–8083.

Mihara, M., S. Erster, A. Zaika, O. Petrenko, T. Chittenden, P. Pancoska, and U.M. Moll. 2003. p53 has a direct apoptogenic roleat the mitochondria. *Mol. Cell*. 11:577–590.

Nagata, E., A. Sawa, C.A. Ross, and S.H. Snyder. 2004. Autophagosome-like vacuole formation in Huntington's disease lymphoblasts. *Neuroreport*. 15:1325–1328.

Ni, Z., B.E. Schwartz, J. Werner, J.R. Suarez, and J.T. Lis. 2004. Coordination of transcription, RNA processing, and surveillance by P-TEFb kinase on heat shock genes. *Mol. Cell*. 13:55–65.

Nishitoh, H., A. Matsuzawa, K. Tobiume, K. Saegusa, K. Takeda, K. Inoue, S. Hori, A. Kakizuka, and H. Ichijo. 2002. ASK1 is essential for endoplasmic reticulum stress-induced neuronal cell death triggered by expanded polyglutamine repeats. *Genes Dev.* 16:1345–1355.

Okazawa, H. 2003. Polyglutamine diseases: a transcription disorder? *Cell. Mol. Life Sci.* 60:1427–1439.

Okazawa, H., J. Shimizu, M. Kamei, I. Imafuku, H. Hamada, and I. Kanazawa. 1996. Bcl-2 inhibits retinoic acid-induced apoptosis during the neural differentiation of embryonal stem cells. *J. Cell Biol.* 132:955–968.

Okazawa, H., T. Rich, A. Chang, X. Lin, M. Waragai, M. Kajikawa, Y. Enokido, A. Komuro, S. Kato, M. Shibata, et al. 2002. Interaction between mutant ataxin-1 and PQBP-1 affects transcription and cell death. *Neuron*. 34:701–713.

Ravikumar, B., C. Vacher, Z. Berger, J.E. Davies, S. Luo, L.G. Oroz, F. Scaravilli, D.F. Easton, R. Duden, C.J. O'Kane, and D.C. Rubinsztein. 2004. Inhibition of mTOR induces autophagy and reduces toxicity of polyglutamine expansions in fly and mouse models of Huntington's disease. *Nat. Genet.* 36:585–595.

Ross, C.A. 2002. Polyglutamine pathogenesis: emergence of unifying mechanisms for Huntington's disease and related disorders. *Neuron*. 35:819–822.

Rubin, G.M., and A.C. Spradling. 1982. Genetic transformation of *Drosophila* with transposable element vectors. *Science*. 218:348–353.

Sapp, E., C. Schwarz, K. Chase, P.G. Bhide, A.B. Young, J. Penny, J.P. Vonsattel, N. Aronin, and M. Difiglia. 1997. Huntingtin localization in brains of normal and Huntington's disease patients. *Ann. Neurol.* 42:604–612.

Saudou, F., S. Finkbeiner, D. Devys, and M.E. Greenberg. 1998. Huntingtin acts in the nucleus to induce apoptosis but death does not correlate with the formation of intranuclear inclusions. *Cell*. 95:55–66.

Schweichel, J.U., and H.J. Merker. 1973. The morphology of various types of cell death in prenatal tissues. *Teratology*. 7:253–266.

Sperandio, S., I. de Belle, and D.E. Bredesen. 2000. An alternative, nonapoptotic form of programmed cell death. *Proc. Natl. Acad. Sci. USA*. 97:14376–14381.

Steffan, J.S., A. Kazantsev, O. Spasic-Boskovic, M. Greenwald, Y.Z. Zhu, H. Gohler, E.E. Wanker, G.P. Bates, D.E. Houseman, and L.M. Thompson. 2000. The Huntington's disease protein interacts with p53 and CREB-binding protein and represses transcription. *Proc. Natl. Acad. Sci. USA*. 97:6763–6768.

Strano, S., G. Fontemaggi, A. Costanzo, M.G. Rizzo, O. Monti, A. Baccarini, G. DelSal, M. Levrero, A. Sacchi, M. Oren, and G. Blandino. 2002. Physical interaction with human tumor-derived p53 mutants inhibits p63 activities. *J. Biol. Chem.* 277:18817–18826.

Sudol, M., H.I. Chen, C. Bougeret, A. Einbond, and P. Bork. 1995. Characterization of a novel protein-binding module – the WW domain. *FEBS Lett.* 369:67–71.

Sugars, K.L., and D.C. Rubinsztein. 2003. Transcriptional abnormalities in Huntington disease. *Trends Genet.* 19:233–238.

Tagawa, K., M. Hoshino, T. Okuda, H. Ueda, H. Hayashi, S. Engemann, H. Okado, M. Ichikawa, E.E. Wanker, and H. Okazawa. 2004. Distinct aggregation and cell death patterns among different types of primary neurons induced by mutant huntingtin protein. *J. Neurochem.* 89:974–987.

Taylor, J.P., J. Hardy, and K.H. Fischbeck. 2002. Toxic proteins in neurodegenerative disease. *Science*. 296:1991–1995.

Terrinoni, A., M. Ranalli, B. Cadot, A. Leta, G. Bagetta, K.H. Vousden, and G. Melino. 2004. p73-alpha is capable of inducing scotin and ER stress. *Oncogene*. 23:3721–3725.

Wyllie, A.H., and P. Goldstein. 2001. More than one way to go. *Proc. Natl. Acad. Sci. USA*. 98:11–13.

Yagi, R., L.-F. Chen, K. Shigesada, Y. Murakami, and Y. Ito. 1999. A WW domain-containing Yes-associated protein (YAP) is a novel transcription co-activator. *EMBO J.* 18:2551–2562.

Zoghbi, H.Y., and H.T. Orr. 2000. Glutamine repeats and neurodegeneration. *Annu. Rev. Neurosci.* 23:217–247.